

# Person Detection Using Ultra-Wideband Radars

## UWB Indoor Person Tracking

by

A. J. van Katwijk,	4334264
A. Šabanović,	4372441
P. P. Verton,	4349725

June 19, 2017

Coordinator: dr. ir. I. E. Lager  
Supervisor: ir. P. Aubry

DELFT UNIVERSITY OF TECHNOLOGY

FACULTY OF ELECTRICAL ENGINEERING, MATHEMATICS  
AND COMPUTER SCIENCE

ELECTRICAL ENGINEERING PROGRAMME  
BACHELOR FINAL PROJECT

This thesis has been prepared with contributions from:

ir. P. Aubry  
dr. ir. I. Lager  
dr. F. Uysal  
prof. dr. A. Yarovoy

Defense Committee:

ir. P. Aubry  
dr. ir. A. J. van Genderen  
dr. ir. I. Lager

# Abstract

In this report, an indoor target detection system is developed for detecting one or multiple targets in a cluttered area based on a network of distributed ultra-wideband radars. The system is capable of acquisition of data in the form of distances between radar and targets, which can be used to localise and track one or multiple targets in real-time. The system can be used in a wide range of applications, ranging from security, such as anti-intruder systems, to commercial applications, such as tracking animals in a zoo.

A network of four Time Domain<sup>®</sup> PulsON<sup>®</sup> 410 ultra-wideband radars are used in the sensing system, due to their availability, high spatial accuracy and performance in non-line-of-sight conditions. By using different transmission codes, interference between the sensors is kept to a minimum. Multiple antennas are considered, and the Vivaldi antenna is shown to be preferred over the dipole antenna for this application due to its slightly higher directivity, reducing the impact of multi-path effects. The data acquisition for the four radars is initiated almost simultaneously, up to the point that the radars can be considered synchronised. The received signal is filtered using background rejection and an FIR motion filter, to reveal motion of the target. Four detection algorithms are considered, of which the least-of constant false alarm rate (LO-CFAR) has a better performance for indoor multiple person tracking applications over conventional CFAR detection. The LO-CFAR algorithm can be applied to the filtered signal to detect targets in range of the sensors, and determine their distance from the sensor. Range-Doppler processing is proposed as a method to acquire a velocity estimate of the target, which can be used in a tracking system to estimate the position of the target more accurately. However, due to the relatively low slow-time sampling frequency, it is not feasible to utilise Range-Doppler processing in the current system. Only simulations of Range-Doppler processing are shown in the thesis.

The system is tested in different environments; single person and multiple person situations are considered in an open and a cluttered area. It is shown that the developed system is capable of detecting a single target in both open and cluttered areas. With two targets in cluttered areas, it becomes difficult to distinguish a target from multi-path reflections, reducing the reliability of the system in these situations. In an open area, multiple targets can successfully be distinguished and detected. The sensing system can successfully detect and determine the distance to a person in non-line-of-sight conditions. Additionally, the detection system is tested on a smaller target to determine performance and accuracy of the system in situations with smaller targets. While the small target is possible to detect, the range at which reliable results are obtained is significantly reduced by the size of the target.

It is concluded that there is room for improvement of the target detection system, especially in situations involving multiple targets in cluttered areas. Through-wall detection is shown to be feasible with the current sensing system. For small targets, a higher pulse integration index is required to achieve a reliable range similar to the results of person detection. Range-Doppler processing requires a higher slow-time sampling frequency in order to be feasible in a real-time tracking system. Further recommendations include testing alternative antennas to improve through-wall detection, designing a multi-static radar system and implementing more complex detection algorithms that have a better multi-person performance.



# Contents

<b>Abstract</b>	<b>iii</b>
<b>List of Figures</b>	<b>vii</b>
<b>List of Tables</b>	<b>ix</b>
<b>Glossary</b>	<b>xi</b>
<b>1 Introduction</b>	<b>1</b>
1.1 Problem Definition . . . . .	1
1.2 Thesis Synopsis . . . . .	2
<b>2 Programme of Requirements</b>	<b>3</b>
2.1 User Requirements . . . . .	3
2.2 System Overview . . . . .	3
2.3 State-of-the-art Analysis . . . . .	4
2.3.1 Passive Sensors . . . . .	4
2.3.2 Active Sensors . . . . .	5
2.4 System Specifications . . . . .	6
<b>3 Hardware</b>	<b>9</b>
3.1 Time Domain® PulsON® 410 Radar . . . . .	9
3.1.1 Radar Description . . . . .	9
3.1.2 Antennas . . . . .	10
3.1.3 Code Channel . . . . .	10
3.1.4 Radar Topology . . . . .	12
3.2 Range Accuracy . . . . .	12
3.2.1 Measurement Methodology . . . . .	12
3.2.2 Results . . . . .	13
<b>4 Data Acquisition</b>	<b>15</b>
4.1 User Interface . . . . .	15
4.1.1 Communication with the Radar Device . . . . .	16
4.1.2 Radar Position and Code . . . . .	16
4.1.3 Radar Parameters . . . . .	16
4.1.4 Data Acquisition . . . . .	17
4.1.5 Scan Display . . . . .	17
4.2 Signal Filtering . . . . .	17
4.2.1 Background Rejection . . . . .	18
4.2.2 Motion Filter . . . . .	18

<b>5</b>	<b>Range Detection Algorithms</b>	<b>21</b>
5.1	Z-score Algorithm . . . . .	22
5.2	Range Compensated Average Threshold . . . . .	24
5.3	Constant False Alarm Rate . . . . .	25
5.3.1	Cell Averaging Constant False Alarm Rate . . . . .	26
5.3.2	Least-Of Constant False Alarm Rate . . . . .	28
5.4	Detection Clustering . . . . .	30
5.5	Discussion . . . . .	32
<b>6</b>	<b>Velocity Estimation</b>	<b>35</b>
6.1	Range-Doppler Processing . . . . .	35
6.2	2-D Velocity Estimation . . . . .	36
6.3	Simulation Results . . . . .	36
6.4	Limitations . . . . .	38
6.5	Improvements . . . . .	38
<b>7</b>	<b>Results</b>	<b>39</b>
7.1	Single Person Detection . . . . .	39
7.1.1	Open Area . . . . .	39
7.1.2	Cluttered Area . . . . .	40
7.2	Multiple Person Detection . . . . .	43
7.2.1	Open Area . . . . .	43
7.2.2	Cluttered Area . . . . .	44
7.3	Through-wall Detection . . . . .	45
7.4	Small Target Detection . . . . .	47
7.5	Results of the Complete System . . . . .	48
7.6	Result Discussion . . . . .	50
<b>8</b>	<b>Conclusion</b>	<b>51</b>
8.1	Reflection on Results . . . . .	52
8.2	Future Work and Recommendations . . . . .	52
	<b>Appendices</b>	<b>55</b>
<b>A</b>	<b>Range Measurements</b>	<b>57</b>
<b>B</b>	<b>Velocity Estimation Using Range-Doppler Information</b>	<b>59</b>
	<b>Bibliography</b>	<b>61</b>

# List of Figures

2.1	Schematic overview of the system . . . . .	4
3.1	Shape of the P410 UWB waveform . . . . .	10
3.2	Dipole antenna radiation pattern . . . . .	11
3.3	Vivaldi antenna radiation pattern . . . . .	11
3.4	Data comparison between Vivaldi and dipole antennas . . . . .	12
4.1	The graphical interface used for interaction with the radars . . . . .	15
4.2	P410 transmit power as a function of Transmit Gain setting . . . . .	16
4.3	Unfiltered scan . . . . .	19
4.4	Motion filtered scan . . . . .	19
4.5	Measurement images at different stages of filtering . . . . .	19
5.1	Image of test data to be used in comparison of detection algorithm . . . . .	21
5.2	Z-score detection results . . . . .	23
5.3	Z-score execution time . . . . .	23
5.4	RCAT detection results . . . . .	24
5.5	RCAT execution time . . . . .	25
5.6	Example of the division of the signal in several range-bins . . . . .	26
5.7	Schematic representation of the CA-CFAR algorithm . . . . .	26
5.8	CA-CFAR detection results . . . . .	28
5.9	CA-CFAR execution time . . . . .	28
5.10	Schematic representation of the LO-CFAR algorithm . . . . .	29
5.11	LO-CFAR detection results . . . . .	30
5.12	LO-CFAR execution time . . . . .	30
5.13	Detection density plot . . . . .	31
5.14	Target clustering of LO-CFAR detection results . . . . .	32
5.15	Target clustering of LO-CFAR execution time . . . . .	32
6.1	Simulated dataset on which the Range-Doppler algorithm will be applied . . . . .	37
6.2	Doppler spectrum of simulated dataset . . . . .	37
7.1	Single-person walking pattern . . . . .	40
7.2	Single-person scan data in an open area . . . . .	40
7.3	Single-person detections and targets in an open area . . . . .	41
7.4	Single-person scan data in a cluttered area . . . . .	41
7.5	Single-person detections and targets in a cluttered area . . . . .	42
7.6	Single-person targets in a cluttered area with a higher minimum detection threshold . . . . .	42
7.7	Multi-person walking pattern . . . . .	43
7.8	Two-person scan data in an open area . . . . .	44
7.9	Two-person detections and targets in an open area . . . . .	44
7.10	Two-person scan data in a cluttered area . . . . .	45

---

7.11	Two-person detections and targets in a cluttered area . . . . .	45
7.12	Through-wall walking pattern . . . . .	46
7.13	Single-person scan data in a through-wall measurement . . . . .	46
7.14	Single-person detections and targets in a through-wall measurement . . . . .	47
7.15	Small target scan data in an open area . . . . .	48
7.16	Small target detections and targets in an open area . . . . .	48
7.17	Target track to be measured by the complete tracking system . . . . .	49
7.18	Tracking results of the complete system . . . . .	49
B.1	Possible velocities for a single Range-Doppler measurement . . . . .	59
B.2	Velocity resulting from the combination of two Range-Doppler measurements . . . . .	60

# List of Tables

I	Scan time and range as a function of the pulse integration index . . . . .	17
II	Parameters of the CA-CFAR algorithm . . . . .	27
III	Algorithm performance in the test measurement . . . . .	33
IV	Used parameters for the PulsON <sup>®</sup> sensors . . . . .	51
V	Accuracy measurement of the P410 radar module . . . . .	57



# Glossary

CA-CFAR	Cell-Averaging Constant False Alarm Rate, a peak detection algorithm.
CUT	Cell Under Test.
EEMCS	Electrical Engineering, Mathematics and Computer Science, a faculty at Delft University of Technology.
Fast-time sampling	Sampling in range.
FFT	Fast Fourier Transform.
FIR	Finite Impulse Response.
LO-CFAR	Least-Of Constant False Alarm Rate, a peak detection algorithm.
P410	PulsON 410 radar module, developed by Time Domain..
PII	Pulse Integration Index.
Pseudo-inverse	The inverse of a rectangular (non-square) matrix.
RCAT	Range Compensated Average Threshold, a peak detection algorithm.
Slow-time sampling	Sampling in time (one fast-time measurements).
UWB	Ultra-Wideband, a wireless technology that uses a large bandwidth to transmit information.



# Chapter 1

## Introduction

### 1.1 Problem Definition

Person tracking technology can be used in many applications. These applications range from security or military applications to more commercial applications. Examples of security applications are anti-intruder mechanisms, airport security systems and through-wall motion detection. A commercial application could consist of providing an organisation (e.g. a store or a museum) with analytic data about the amount of visitors and their motion, or tracking the position and motion of animals in a zoo.

The challenge of person tracking can be divided into two parts: target detection and target tracking. Target detection focuses on sensor data acquisition, and processing the received data in order to estimate the distance to the target. Target tracking includes localising the target, error rejection and tracing the path of the target. This thesis will focus on the detection of moving targets.

In order to successfully track a target, a good detection is desired. Although the hardware used for sensing targets may differ between different types of tracking systems, the general idea remains the same: the signal received from the sensing system needs to be interpreted and processed in such a way as to obtain an estimate of the distance between the sensor and the target.

Aside from the location of the target, it is beneficial for target tracking if the velocity of the target can be determined. By estimating both the speed and the direction of movement of the target, the next location of the target can be predicted. This has the potential to improve the accuracy of target tracking and to resolve ambiguous situations such as crossing paths in situations involving multiple persons.

Based on the definition of the problem, the following goals can be distinguished for the desired detection system:

- Designing a sensing system to detect and track human beings in indoor environments.
- Writing data acquisition software.
- Pre-processing and filtering the received signal.
- Implementing a target detection algorithm.
- Implementing a target velocity estimation algorithm.

The body of the thesis is divided based on these goals.

## 1.2 Thesis Synopsis

In this thesis, the design steps and signal processing necessary for target detection using a distributed network of sensors are described. First, a programme of requirements with user requirements and technical specifications is given in Chapter 2. In Chapter 3, the used hardware is described and evaluated. The user interface, data acquisition and signal filtering is introduced in Chapter 4. The target detection algorithms used for determining the distance between the sensor and the target are discussed in Chapter 5. Target velocity estimation is described in Chapter 6. A discussion of the test results for the detection system is shown in Chapter 7 and, finally, a conclusion including future work and recommendations is given in Chapter 8.

## Chapter 2

# Programme of Requirements

In Section 1.1, the problem of person tracking has been defined. This chapter will focus on the technical specifications, which are derived from the user requirements. A summary of the user requirements is given in Section 2.1, followed by an overview of the tracking system in Section 2.2. A state-of-the-art analysis on sensor types is shown in Section 2.3, in order to determine which sensor type is capable of meeting the user requirements. Based on the state-of-the-art analysis, a sensor type is selected and the user requirements are translated to technical specifications of the system. The derivation of the technical specifications is discussed in Section 2.4.

### 2.1 User Requirements

Based on the problem definition in Section 1.1, a tracking system has to be designed and implemented that satisfies the user demands and the requested functionality of the system. These user requirements are summarised below.

1. The system must be able to detect and track one or two persons in an area of interest.
2. The system must be able to perform tracking in real-time, providing at least 5 locations per second for each target.
3. The system must be able to track persons in cluttered areas and non-line-of-sight conditions.
4. The determined location of a person must be accurate within 15 cm.
5. The system must be able to determine the velocity of a person up to  $2 \text{ ms}^{-1}$ .
6. The system must be operable through a central control unit.
7. The system must be able to operate continuously without the intervention of users.
8. The sensing system must be able to cover an area of 6x6 metres.
9. The sensing system must be mobile with a set-up time of at most one hour.
10. The average power consumption of the sensing system must not exceed 50 W.

### 2.2 System Overview

In order to detect and track persons, a sensing system is required. A central unit collects information from the sensors, processes it to detect human beings, determines their positions and maintains the track of each person. The positions are communicated either to a human operator or to a higher level system.

An overview of the system is schematically represented by Fig. 2.1. In the overview, a distinction is made between the hardware, consisting of the sensing system, and the signal processing software used to interpret the data. The arrows represent the data flow, and the numbers represent the type of data that is passed between processing stages. The system is initiated through user input, which enables the data acquisition. In this step, communication is established with the sensing system. From the central unit, parameters can be specified by the user, which can be transmitted to the sensors. After all the parameters have been set, data can be requested in order to initiate the measurement. The detection of targets starts with the required signal processing, such that the detection algorithm can use the processed signal to determine whether a person is present in the vicinity of the radars. If one or multiple persons are present, the distance between the radar and each target is determined. These distances are required by the tracking module in order to determine the target locations and trace the path of each target. The tracking module is discussed in [1] and will not be further discussed in this thesis. A velocity estimation of the target is made to further improve the accuracy and reliability of the tracking system.

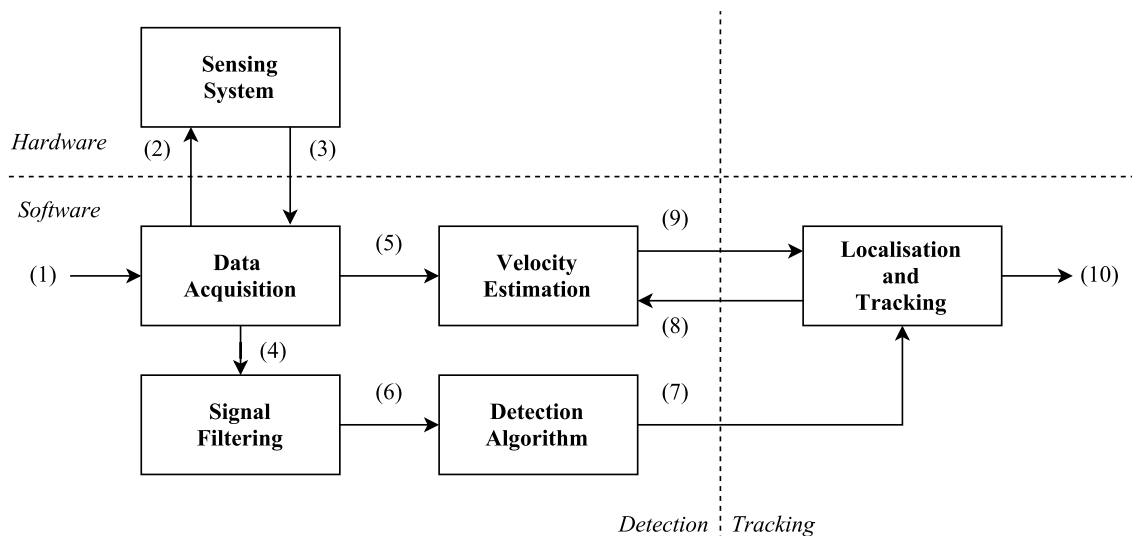


Fig. 2.1: Schematic overview of the system. The arrows represent flow of data: (1) user input, (2) commands to sensing system, (3), (4) and (5) raw signal, (6) filtered signal, (7) detected target distance, (8) target location, (9) target velocity estimation and (10) target position and track output.

## 2.3 State-of-the-art Analysis

In order to assess which type of sensor is preferred for tracking applications described by the user requirements, several options are considered. Many implementations of tracking systems already exist, each with their own advantages and disadvantages. When considering sensor types, two main categories can be distinguished: passive and active sensors. From each category, some feasible sensor types will be considered in Section 2.3.1 and Section 2.3.2, in order to choose the optimal sensor that meets the user requirements. This sensor type will in turn be used in the remainder of the implementation of the detection system.

### 2.3.1 Passive Sensors

Passive sensors observe the environment without the use of a transmitter or source. They rely solely on the environment and its observability. The advantage of this is that this type of sensor cannot be directly detected by others, since they do not transmit any information. However, by only relying on the environment to make detections, instead of using a transmitter, situations exist where passive detection cannot be applied. The advantages and disadvantages of several types of passive sensors will now be discussed.

### Optical Sensors

Optical sensors rely on optical visibility of the environment. A well known example of passive optical sensors are cameras. The advantage of optical sensors is that some tracking implementations already exist [2], and many types of optical sensors are readily available. However, in poor visibility conditions, such as fog or smoke, cameras have a bad performance. Another disadvantage is that, with multiple targets, shadowing will occur, where one target will be (partially) invisible due to another target in front of it. Aside from this, cameras are mainly used for identification or simply detection, as tracking target locations is difficult without the aid of other types of sensors. Finally, cameras require direct line-of-sight on the target in order to detect it, which means that through-wall applications are not feasible. This makes cameras undesirable for indoor person tracking.

### Infrared Sensors

Another type of passive sensor are infrared sensors. Their performance in terms of resolution and target classification is generally higher than that of cameras and do not require external illumination of targets. [3] Furthermore, they have the advanced capability to distinguish between human beings and environment using temperature differences. However, infrared sensors would be blinded by larger heat sources, such as fires. Similarly to cameras, infrared sensors require direct line-of-sight on the target, which makes tracking in indoor environments more difficult, and does not meet the user requirements.

### Pressure Sensors

Pressure sensors can be used to detect the presence of targets using the force applied to them. With the use of multiple pressure sensors, tracking becomes trivial, as the position of a target can be determined directly by the position of the pressure sensors that are activated by the target. With sufficient resolution, footprints could even be used to distinguish several targets, and associate them to a path, such as in [4]. However, the disadvantage of this implementation is that the tracking system has to be installed ahead of time in order to hide the sensors from other parties, making it an immobile sensing system. Aside from this, a large amount of hardware is required to cover an area, especially if a high spatial resolution is required, which could have a big impact on the costs of such an implementation.

### Acoustic Sensors

Acoustic tracking systems use microphone arrays to detect targets using, for example, time-distance-of-arrival algorithms, such as in [5] and [6]. Unfortunately it is highly susceptible to noise, an additional sound source can already give rise to difficulties in detecting the initial target. Therefore, it is difficult to detect persons using passive acoustic sensors, and a tracking system based on this type of sensor would likely be unreliable.

## 2.3.2 Active Sensors

Active sensors use a transmitter and a receiver to determine whether a target is present in a certain area. For this, time-of-arrival can be used, by transmitting a signal and receiving its reflections, such that information about the environment can be obtained. This transmitted signal could possibly be detected by external parties, which could be an issue in security applications. However, using active sensors can greatly improve the possible ways to detect targets. Several types of active sensors are now discussed.

### Laser Sensors

Laser tracking systems, such as laser grids or LIDAR (LIght Detection And Ranging), are a form of active optical sensors that transmit a light pulse, receive reflections, and determine distances to objects or targets. Lasers are already used for person detection [7], and LIDAR has been utilised for creating high-resolution images of an environment. [8] Both sensors suffer from shadowing, where one target blocks visibility of

the area behind him. On top of that, because both sensors are optical, they will have a poor performance in low visibility areas, and require a direct line-of-sight in order to observe the target.

### RFID Sensors

Radio Frequency Identification, or RFID, uses beacons or 'tags' that can be detected using radio frequency transmission and reception, such as in [9]. The tags used in RFID tracking systems allow for identification of targets, such that their tracks are separable. Due to the use of radio frequencies, non-line-of-sight or even through-wall applications are feasible. However, a disadvantage of this implementation is that each target would be required to carry such a tag, reducing the possible tracking applications. For example, for security systems, targets with such a tag would be visible, while intruders without these beacons would not.

### Radars

Radars have several advantages in multiple situations compared to the previously mentioned sensors, such as in areas with limited view conditions. Several radar types exist, such as narrow-beam radars, which rotate steadily while sweeping the area with a narrow beam. [10] However, the large size of narrow-beam radars are not particularly well-suited for indoor tracking applications. Another important radar type is the ultra-wideband (UWB) radar, which uses a large bandwidth to transmit information. Among the different radar types, UWB radars are particularly useful for person tracking in indoor applications because of its high range resolution, offering high precision localisation and the ability to distinguish multiple adjacent targets, which enables the ability to track multiple persons. [11] The major advantage of radar-based tracking systems over other types is that a direct line of sight is not necessary for detection, which enables through-wall detection and tracking. [12] [13] [14] This makes radar technology well-suited for indoor applications. The possibility of using radar technology for detection and tracking applications has been demonstrated several times, such as in the research done in [15] and [16]. A disadvantage of radar-based tracking systems is that multi-path reflections play a large role in the accuracy of the system. This is especially a problem in cluttered rooms. However, by using information about the received background signal and signal filtering, it is possible to limit multi-path effects. For these reasons, radars are considered to be an excellent sensor type for tracking applications, both in outdoor and indoor environments. In this thesis, radars will be used to implement a target detection system.

## 2.4 System Specifications

The user requirements described in Section 2.1 can be transferred into system specifications in order to properly assess the design problem. These specifications will be derived in this section based on the use of radar technology in the sensing system, which was determined in Section 2.3 to be the preferred sensor type for indoor tracking applications.

### Multiple Person Tracking

In order to realise real-time person tracking in an area of interest, the area should be properly covered by the range of the sensor. One way to realise this is by using a narrow-beam radar to track persons in the area. However, this would require a large radar structure, reducing the mobility of the sensing system and making indoor person tracking difficult to realise. A distributed network of small, omnidirectional radars are more effective at covering an area quickly, while also allowing for easy setup and transport of the sensing system. With a network of small radars, indoor person tracking becomes more feasible.

With a distributed network of sensors, at least three sensors nodes are required to prevent ambiguity in the location of a person. Such a system is called an overdetermined system. According to the user requirements, the system must have the ability to detect and track one or two persons. This means that a sensing system consisting of at least four nodes is required to maintain a determined system, and to prevent ambiguity in target positioning. [17]

## Non-line-of-sight Detection

Detection of persons in cluttered or non-line-of-sight conditions requires the ability to sense persons through objects, such as plants, tables or walls. This requirement puts a restriction on the frequency of the signal, because higher frequencies have more difficulty penetrating objects due to the larger wave attenuation inside the object. Relatively low frequencies like mobile communication frequencies are more feasible for through-wall detection, such as the Wi-Fi frequencies of 2.4 GHz and 5 GHz. Frequencies in the X band (8 to 12 GHz) and above are mostly used for line-of-sight applications due to the large attenuation in materials. [18] Therefore, a technical specification is made which restricts the maximum frequency of the sensor to 8 GHz.

## Location Accuracy

In order to determine the location of a target within an accuracy of 15 cm, a large bandwidth is required to achieve a short time-domain pulse. The range resolution of a radar is given by Eq. 2.1. [19]

$$S_r = \frac{c}{2B} \quad (2.1)$$

Here,  $S_r$  is the range resolution of the radar,  $B$  represents the bandwidth of the radar and  $c$  is the speed of light. From this equation, it can be derived that a bandwidth of 1 GHz is required to realise a range resolution of 15 cm. However, when determining the location of a target in realistic applications, the error made by the radar will generally be worse. Therefore, a bandwidth larger than 1 GHz is required in order to guarantee that the location accuracy requirement is met. In order to meet this requirement, ultra-wideband radars can be used. UWB radars spread information over a large bandwidth ( $> 500$  MHz), and are therefore suitable for implementing tracking systems with high spatial resolution.

## Detection Accuracy

A requirement on the detection accuracy of the detection algorithm can be placed. The detection accuracy specifies the number of detections that are correctly made on the position of the target(s). The number of false detections and missed detections must be kept as low as possible. According to [1], in order to have reliable tracking of a target, at least 60% of the locations must be correct, and the number of consecutive missed locations must not exceed five. For the detection algorithm, this means that at least 60% of the path of the target must be correctly detected, and no more than five consecutive missed detections may occur.

## Sensor Range

Based on the requested size of the area of interest, each sensor in the sensing system is required to provide reliable measurement data up to at least 8.5 metres, assuming that each sensor is placed on the corner of a square-shaped area. By using a range of 8.5 metres for each sensor, the entire requested area of 6x6 can be observed.

## System Refresh Rate

The refresh rate of the system is determined by the measurement time and the time required to process data. In order to provide five locations per second, the measurement time and processing time combined must not exceed 200 ms.

## Central Control Unit

A central control unit is requested by the user, which can control all parameters of the sensing system and controls the tracking system. All inputs must be adjustable from this control unit, and the output of the tracking system should be accessible by the control unit. Therefore, an application must be developed that contains an interface with adjustable parameters for the sensing system, shows the current location of any target in the area of interest and stores the track history of previous targets in an archive.

## Summary

In the previous sections, technical specifications for the detection system have been derived from the user requirements. These technical specifications are summarised below.

1. The sensing system needs to contain at least four nodes.
2. The bandwidth of the radar must be larger than 1 GHz.
3. The operational frequency of the sensor should be below 8 GHz.
4. The system must detect persons within 30 cm of their centre position.
5. The sampling and processing time must not exceed 200 ms.
6. The sensing system must be controlled from a single central control unit.
7. The sensors are required to have a range of at least 8.5 metres.
8. At least 60% of the detections made by the detection algorithm must be correct, and at most five consecutive detections can be missed.
9. The velocity estimation algorithm must be able to determine target velocities up to  $2 \text{ m.s}^{-1}$ .
10. The average power consumption of the sensing system must be at most 50 W.

# Chapter 3

## Hardware

This chapter discusses the hardware used to acquire the measurements. First, in Section 3.1, a choice is made on which sensor to use in order to meet the technical specifications. Then, the sensor and its extensions are put into perspective. Finally, results of accuracy measurements of the selected sensor are shown in Section 3.2.

### 3.1 Time Domain<sup>®</sup> PulsON<sup>®</sup> 410 Radar

Based on the technical specifications, an ultra-wideband radar with a low-end frequency of 3.1 GHz and a bandwidth of 2.2 GHz is chosen, which is in accordance with the technical specifications. Four radar modules were made available for testing by the Microwave Sensing department of the EEMCS faculty of the Delft University of Technology. A description of the radar module is given below.

#### 3.1.1 Radar Description

The radar used in this implementation is a Time Domain<sup>®</sup> PulsON<sup>®</sup> 410 (P410) module. This module transmits a pulse with a high bandwidth and records the received waveform as its reflections return. From the time-of-arrival of these reflections, the distance to a target can be determined. The P410 has a frequency range from 3.1 to 5.3 GHz, with a centre frequency of 4.2 GHz. Figure 3.1b shows how the power is distributed over these frequencies. To prevent interference between multiple units, pseudo-random encoding is used. The device samples the received waveform in steps of 1.907 ps, of which 32 are internally averaged, resulting a sampling time of 61 ps. Since the two-way distance is measured, a range accuracy of 9.16 mm per sample is obtained. This is sufficient to meet the required accuracy.

The high bandwidth of the radar allows for a very narrow pulse. The advantage of a narrow pulse is that it gives sharp peaks for clutter in the environment, allowing them to be suppressed using simple filters. This clutter rejection makes the UWB nature of the radars excellent for indoor environments. The large bandwidth enables a very short pulse waveform of only 1 ns, which is shown in Fig. 3.1.

Another advantage of the P410 is its low power usage. With a peak power consumption of 4.2 W, which can be reduced to 1.1 W using a sleep mode, as shown in the datasheet [20], the sensing system can consist of up to 11 radar modules while still meeting the power specification preferred by the user. This low power usage makes the system cheap to operate and enables powering of the devices using batteries for short-term usage. The power emitted in a pulse can be customised, as it is adjustable without changing the hardware. The transmitted power can be adjusted from -31.6 to -12.64 dBm or, with an optional high-power amplifier, from -14.5 to 0.7 dBm.

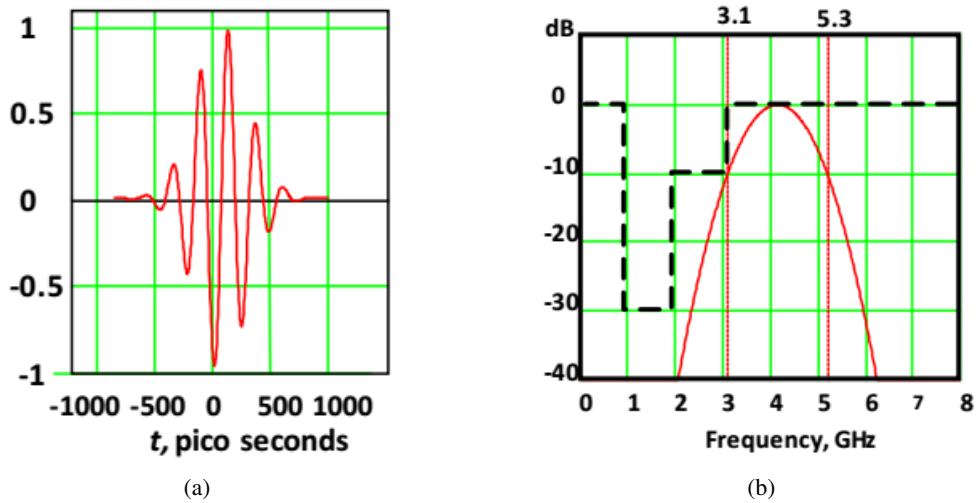


Fig. 3.1: P410 UWB waveform in (a) time domain and (b) frequency domain. Figures taken from [20].

### 3.1.2 Antennas

To transmit the pulse generated by the P410, an antenna is required. By default, the P410 is equipped with a pair of dipole antennas. With the supplied antennas, multi-path reflections have a large impact on the received signal. This is due to the omnidirectional nature of the supplied antennas. For this reason, a more directional set of antennas is preferable.

The radiation pattern of two available antennas are considered in order to choose the most suitable antenna type for this application. Figure 3.2 and Fig. 3.3 show the radiation patterns of both antenna types at different frequencies. The Vivaldi antenna clearly shows a more directional nature with a reduction of up to 4 dB on waves incident at from the left side.

Figure 3.4 shows the result of a measurement using both antenna types. The x-axis shows different measurements in the time-domain, hereafter referred to as slow-time samples, and the y-axis shows the distance from the radar, from now on referred to as fast-time samples. A yellow colour corresponds to a high intensity of the measured signal, while a blue colour indicates a low intensity. The images show a person moving towards and away from the radar from several angles. On the right side of the image, the person approaches the radar at a 180 degree angle. The left side of the dipole measurement (Fig. 3.4a) shows that there is a high intensity multi-path reflection around 4 metres. This reflection is a lot less visible in the Vivaldi measurement, which is likely because of the directivity of the Vivaldi antenna. The measurement with a Vivaldi antenna also shows a smaller signal amplitude when the person is located behind the radar, which is beneficial in applications where the area of interest is directly in front of the radar, rather than surrounding the radar.

### 3.1.3 Code Channel

To prevent interference between multiple radar devices, code channels are implemented. Pulses are encoded and spaced pseudo-randomly in order to make the transmissions noise-like and prevents interference between multiple devices. The noise-like transmissions also make sure that other parties cannot easily intercept the transmitted signals. Currently, seven different code channels are available, allowing operation of seven radar devices in range of each other without interference.

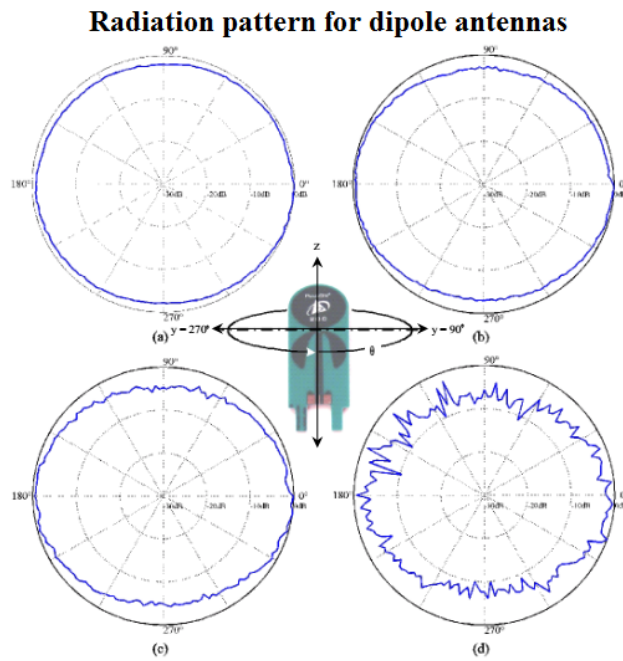


Fig. 3.2: Dipole antenna radiation pattern for (a) 3 GHz, (b) 4 GHz, (c) 5 GHz and (d) 6 GHz. Figure taken from [21].

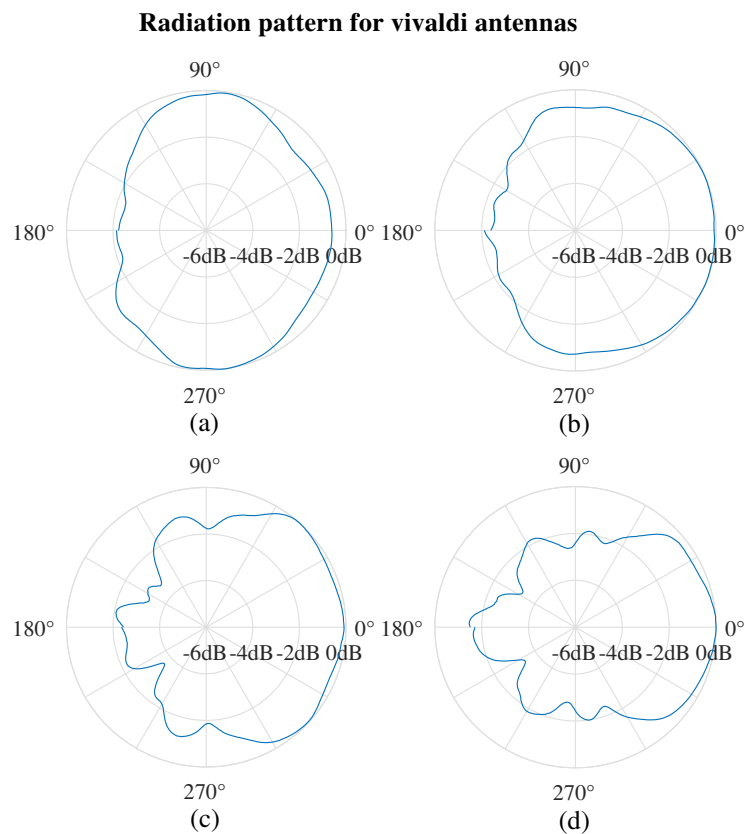


Fig. 3.3: Vivaldi antenna radiation pattern for (a) 3 GHz, (b) 4 GHz, (c) 5 GHz and (d) 6 GHz.

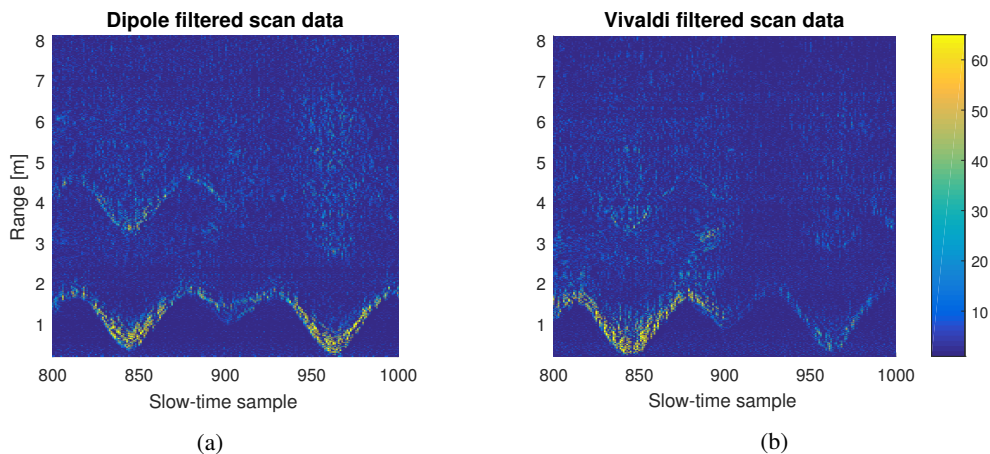


Fig. 3.4: Filtered data of the dipole antenna (a) and the Vivaldi antenna (b).

### 3.1.4 Radar Topology

In order to satisfy the user requirement for area coverage, a radar topology has to be chosen which can effectively detect any target within the area with a minimum amount of hardware used. In the ideal case, three sensors are enough to determine the two-dimensional location of a target, regardless of target position. However, the P410 sensors have a minimum range to detect a target. This is caused by direct coupling between the transmitting and receiving antennas. These reflections make it difficult to detect targets within one metre of the radar module. In a topology with only three sensors, this would cause a blind spot near each radar module where only two radars could detect the target, resulting in ambiguity in the location of the target. To prevent this, a fourth radar is required such that there will always be at least three radars that are able to detect the target. In addition, to avoid most ambiguous situations when two persons are involved, four sensors are required, as explained in 2.4. Since at least four sensors are required according to

the technical specifications, and because the area of interest is at most 6x6 metres, a square or rectangular topology consisting of four sensor nodes on each corner can be used to maximise the covered area while minimising the required hardware.

## 3.2 Range Accuracy

To determine the accuracy of the tracking system, it is important to know the accuracy of the individual radar modules.

### 3.2.1 Measurement Methodology

To measure the accuracy of the radars, a large metal plate is placed at certain distances from the radar. Because of the high reflectivity of the metal plate, this will result in a large narrow peak in the received radar signal. The position of the metal plate can then be accurately determined both using a laser measure and from the position of the peak in the received radar signal. The peak position can be compared to the manually measured distance to determine the accuracy.

A laser measure with a resolution of 1 mm is then used to determine the actual distance to the plate, and the difference between the two measurements is determined. By doing this for multiple distances for the plate, any systematic and random errors in the radar distance measurement are determined.

### 3.2.2 Results

The results of these measurements can be found in Appendix A. From these results it is determined that the measured range from the radar detection is, on average, approximately 9 cm smaller than the measured range from the laser measure. The reason for this deviation is possibly caused by the difference in position of the laser measure and the phase centre of the radar antenna, or by a systematic offset within the radar module.

Additionally, a random error with a standard deviation of about 4 cm is observed. The assumption is made that this is caused by the inaccuracy of the used detection algorithm, as well as random variations in the measured radar signal.



# Chapter 4

## Data Acquisition

In this chapter, the process of acquiring and pre-processing data is explained. First, a user-friendly MATLAB interface is introduced in Section 4.1, through which the sensing system can be controlled. In Section 4.2, the steps in signal filtering are explained, which consist of background rejection and motion filtering.

### 4.1 User Interface

For the user, it is important that an interface is available which contains all the required controls and indicators in order to be able to properly detect and track targets in a certain area. This graphical user interface is developed in MATLAB and is shown in Fig. 4.1. Several parts of the interface are discussed below.

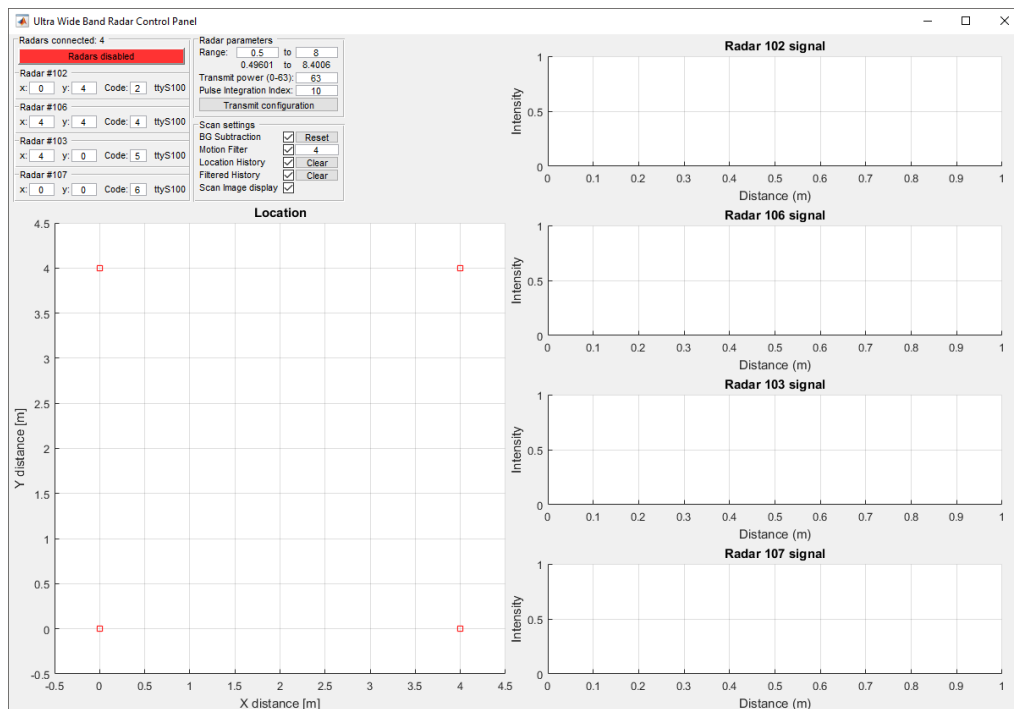


Fig. 4.1: The graphical interface used for interaction with the radars.

### 4.1.1 Communication with the Radar Device

Communication with the radars is done through simple USB messages which are detailed in the API specification. [22] Each message is confirmed by the radar with a status indication, which allows for error detection. Scanning on the radar is started by transmitting a certain message to the radars. The radars confirm this message and start scanning internally. When scanning is completed, the radars transmit the scan data in a set of several packages.

### 4.1.2 Radar Position and Code

The top left section of the interface allows adjustment of radar locations. This allows different radar arrangements and distances. The radar code defines which encoding it uses in its pulse, allowing for operation of multiple radar devices without cross-interference. The code channels have been discussed in Section 3.1.3.

### 4.1.3 Radar Parameters

Next to the radar positions, the parameters used for the scan on the radar device can be adjusted. The range can be set to determine how many fast-time samples are to be taken by the radar. A higher range will therefore increase measurement time, but also reveal a larger area to the radar. Since the radar can only measure in intervals of 96 samples, the range specified will not be the exact range on the radar. The exact range is shown just below the desired range.

Transmission power is specified in a number from 0 to 63, which corresponds to a transmit power of -31.6 to -12.64dBm. [20, Tbl.2] Figure 4.2 graphically shows the transmitted power for different settings.

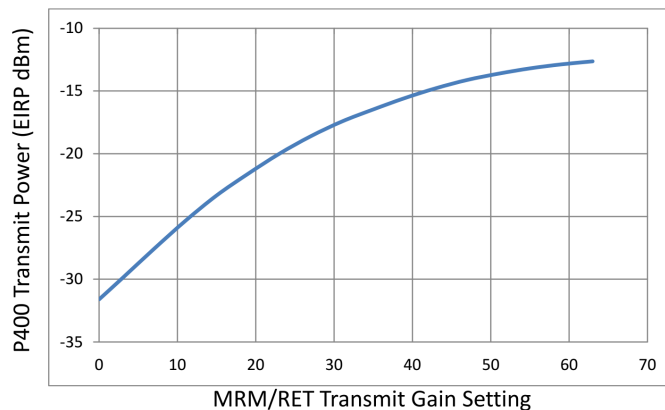


Fig. 4.2: P410 transmit power as a function of the Transmit Gain setting. Figure taken from [20].

Integration is done over several scans to increase the signal-to-noise ratio. The number of scans used per measurement are defined by the Pulse Integration Index (PII).  $2^{PII}$  scans are integrated, with an increase in signal-to-noise ratio of 3 dB with increment of the PII. This gives a dynamic range of 30 to 75dB. [20, Tbl.2] Increasing the PII also increases the scan time and the maximum reliable range of detection in line-of-sight conditions, as seen in Table I. Scan times were obtained by averaging the time required for 1500 scans. The table shows that a PII of 14 or 15 will not provide a refresh rate of 5 Hz, and therefore do not meet the user requirements. The maximum usable PII which is in accordance with the required refresh rate is 13.

For non-line-of-sight conditions, the maximum reliable range must be determined empirically, since different materials have different penetration depths. For a pulse integration index higher than 11, determining the maximum range becomes difficult due to limited room sizes for testing. Therefore, a minimum range is supplied for a PII of 12 or higher.

Table I: Scan time and range as a function of the pulse integration index.

PII	1 radar		4 radars		Range [m]
	Time [ms]	Sample rate [Hz]	Time [ms]	Sample rate [Hz]	
7	21.93	46.6	57.81	17.3	4
8	23.82	42.0	57.53	17.4	6
9	27.86	35.9	60.79	16.5	8
10	52.25	19.1	80.30	12.5	9
11	64.07	15.6	88.90	11.2	10
12	92.64	10.8	128.8	7.80	>10
13	152.7	6.54	188.2	5.31	>10
14	273.0	3.66	304.9	3.28	>10
15	513.5	1.95	536.8	1.86	>10

#### 4.1.4 Data Acquisition

The data acquisition can be initiated by enabling the radars using the enable button. After calibration, which is discussed in Section 4.2, the detection, localisation and tracking immediately starts. If at least three radars detect a possible target, the localisation is attempted, which is immediately shown in the graph on the bottom left of the interface. Both the location history and the tracking history can be enabled, disabled and cleared.

Since the scanning takes time and is done on the radar devices itself, the processing of the previous data can be done whilst the radar is scanning. This is done by starting the scan on the radar, processing the data of the previous scan, and then retrieving the scan data from the USB buffer for the next cycle.

The data that is acquired from the radars must be synchronised to be able to properly convert ranges into locations. This is done by transmitting the request to start scanning at the same time, before waiting for a reply. This ensures the radars start scanning within a millisecond of each other.

#### 4.1.5 Scan Display

On the right side of the interface, the four radars and their filtered fast-time data are shown. The user has the option to switch this graph to an image that shows the slow-time/fast-time data of the past 500 measurements. This image is often more useful, as it reveals clearly what the radars have measured over the past 500 measurements, which could reveal information to the user that might not have been included in the location graph. The display format can be changed using the "Scan Image Display" checkbox, which toggles between one or multiple slow-time measurements. Figure 4.3 shows an example of raw scan data obtained from a radar. After filtering and applying a detection algorithm, the graph of Fig. 4.4 is obtained, which clearly shows a distinct peak at 5m, where a moving person is located. Figure 4.5c shows the image of several slow-time measurements, where yellow indicates high intensity areas and blue indicates low intensity areas. The intensity is given in arbitrary units. The image shows a person moving towards and away from the radar.

## 4.2 Signal Filtering

The received signal contains, besides information about any present targets in the vicinity, noise due to atmospheric noise, reflections from clutter in the environment, and direct coupling between the antennas. Before any information can be obtained from the scans, the data must be filtered. The goal of the filtering is to reduce the impact of static objects and clutter in the environment which could otherwise cause an incorrect detection in the range detection stage, which is detailed in Chapter 5. The filtering is done in two stages. First, background rejection as described in Section 4.2.1 is used to remove the static objects from

the signal. Then, a motion filter is applied to further suppress static clutter and to remove static objects that have moved slightly, such as the of a room. The motion filter is described in Section 4.2.2.

Figure 4.5a shows the data as obtained by the radar. Measurement starts simultaneously with the transmission of the pulse, which causes high-intensity coupling between the two antennas, which are at a distance of 4 cm from each other. This coupling causes a very high intensity signal to be received in the first 0.5 m of the received data. Horizontal stripes are also visible, which are caused by reflections from static clutter in the environment. The image also shows a person moving closer and then moving away. The intensity of many of the static reflections is higher than the signal received from the reflections of the person, so the person is practically undetectable without signal filtering. A single scan is shown in Fig. 4.3. In this scan, the person around 4.5m is unobservable due to the reflections of walls and different objects in the environment.

### 4.2.1 Background Rejection

To reduce the effect of static objects and direct coupling between the antennas, background rejection is applied. Scans of the environment without present targets are stored and the average of those scans is subtracted from all subsequent scans, in order to calibrate the radars to the environment. With the refresh rate of around 10 Hz, a three second calibration results in 30 scans being used for the background rejection. This removes the effect of the direct coupling between the antennas and also removes significant peaks due to clutter in the environment. However, some objects, such as doors, are not completely static and can therefore change the background of the environment when moved.

Figure 4.5b shows the result after background rejection. The left side of the image shows the training period of 30 scans, after which the high intensity horizontal lines present in Fig. 4.5a are completely suppressed. The movement of the person is clearly visible. Near the 50th scan reflections appear around 6 meters, presumably due to a slight change in a static object in the environment. The intensity of these slight changes can become higher than the desired signal due to the person. To reduce the effect of these occurrences, a motion filter is required that can effectively distinguish a moving target from the background.

### 4.2.2 Motion Filter

To further reduce the effect unwanted reflections on the signal, a motion filter is used. The motion filter is implemented as a Finite Impulse Response (FIR) filter. Equation 4.1 shows the basic equation of an FIR filter, where  $y[n]$  represents the filtered signal,  $x[n]$  represents the raw signal. By subtracting past measured samples from the new sample, a motion filter can be implemented. An FIR filter is chosen due to its algorithmic simplicity and low processing cost. The length of the FIR filter determines how quickly movements are suppressed and also how much of an effect an object has on subsequent scans. If the order is too high, a person moving past a point might influence the measurement long after they have left the area of interest, and could therefore interfere with the detection of a different target. If the order is too low, even fast movements will be suppressed and slow-moving targets will be undetectable. A low order has the advantage that quasi-static objects are quickly suppressed after they have moved.

$$y[n] = x[n] + \sum_{i=1}^N a_i \cdot x[n - i] \quad (4.1)$$

A fourth-order FIR filter is found to be a good trade-off between suppression speed and minimum motion velocity. The coefficients used in the implementation of the motion filter are shown in Eq. 4.2. These coefficients give full suppression of static objects after 4 scans. Some experiments were done with different lengths and coefficients such as coefficients dropping with a  $1/x$  or  $1/x^2$  characteristic, but these did not improve the results and are computationally more expensive.

$$y[n] = x[n] - 0.6x[n - 1] - 0.3x[n - 2] - 0.1x[n - 3] \quad (4.2)$$

It is considered that a motion filter might attenuate the signal amplitude of slow-moving targets. With a fourth-order FIR, a target only needs to move through two to three fast-time samples per scan to be detected. With a PII of 11, the sample rate is around 11 Hz. Since the range accuracy is 9.16 mm, a person would have to move each part of themselves slower than 10.1 cm per second to avoid detection.

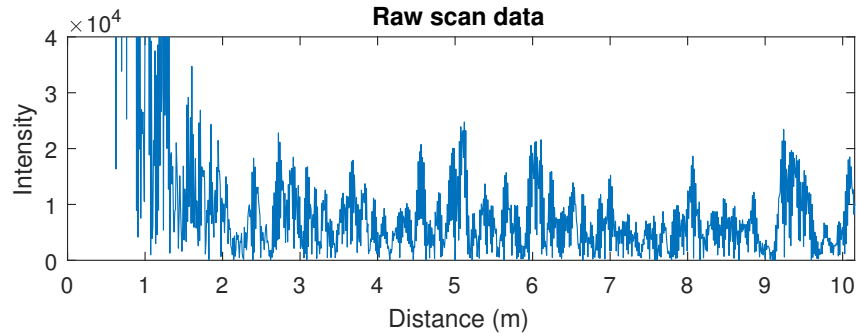


Fig. 4.3: A single unfiltered scan. The person at 4.5m is invisible due to noise in the signal.

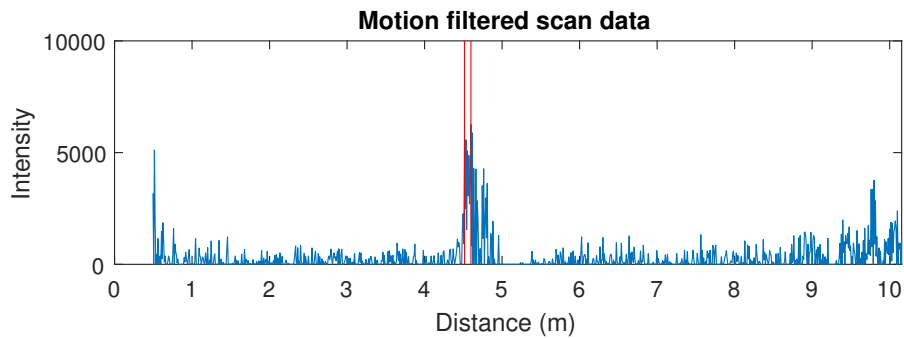


Fig. 4.4: A single filtered scan. The person at 4.5m is clearly visible and two detections are made.

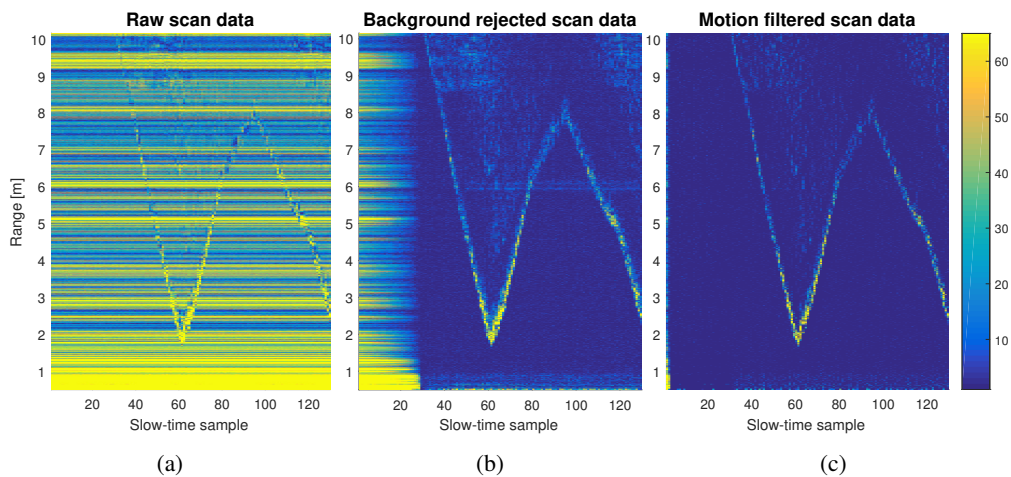


Fig. 4.5: Measurement images at different stages in filtering: (a) raw data, (b) with background rejection and (c) with background rejection and motion filtering. Measurements taken with a Pulse Integration Index of 11. Yellow shows high-intensity areas.



## Chapter 5

# Range Detection Algorithms

Now that the received signal is filtered, as described in Chapter 4, detection algorithms can be used to interpret the measurement data and determine the distance between the sensor and the targets. In this chapter, several detection algorithms and their performance are discussed. The designed algorithm should have the ability to detect clear peaks in the signal, which would indicate a target, while ignoring peaks from noise and multi-path propagation as much as possible. The detection algorithms are discussed in Section 5.1 through 5.3. Detection clustering and linking multiple detections to isolated targets is discussed in Section 5.4, and a final comparison between the several detection algorithms is shown in Section 5.5. In order to compare the detection algorithms in terms of execution time, detection accuracy and robustness, a test measurement is made on which the algorithms are applied. The radar range image of the data that is used for testing the algorithms is shown in Fig. 5.1. In this measurement, the motion of one target is clearly visible, and no other targets are present, which means that (preferably) no detections are made outside of this path. The maximum range in the test measurement is set to 8 metres.

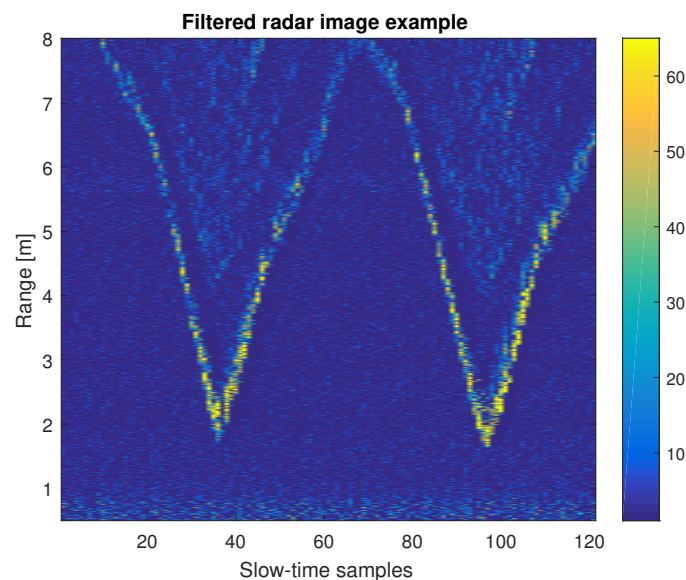


Fig. 5.1: A test image from a person walking in a square in front of the radar. This data is used in the comparison of several detection algorithms.

## 5.1 Z-score Algorithm

The z-score algorithm, or standard score algorithm, uses the average and standard deviation of fast-time samples in the signal  $x[n]$  to calculate whether a peak is present in the sample under test or not. [23] The mean value  $\mu$  of the previous  $N$  samples of signal  $x[n]$  is given by Eq. 5.1, and the standard deviation  $\sigma$  is given by Eq. 5.2.

$$\mu = \frac{1}{N} \sum_{i=1}^N x[n-i] \quad (5.1)$$

$$\sigma = \sqrt{\frac{1}{N} \sum_{i=1}^N (x[n-i] - \mu)^2} \quad (5.2)$$

### Algorithm Process

In order to determine whether a sample corresponds to a peak or not, a threshold is required as a reference. In the z-score algorithm, to determine whether a sample in the signal is a detection, the average and the standard deviation of the preceding  $N$  samples are calculated and used to determine the threshold. If the amplitude of the test sample deviates several standard deviations from the moving average, a peak is present at the test sample. The mathematical representation of this threshold  $\alpha$  is shown in Eq. 5.3, where  $c$  represents a constant scale factor.

$$\alpha = \mu + c \cdot \sigma \quad (5.3)$$

### Parameters

The z-score algorithm has two main parameters that can be set. The first parameter to consider is the lag, which sets the number of preceding samples used in the calculation of the average and the standard deviation. By increasing the lag, the adaptation speed of the algorithm is decreased, since the average and the standard deviation will change more slowly. However, a larger lag also means that more computational power is required, resulting in a slower algorithm. It is also important to note that a large lag may cause a large peak to 'shadow' a smaller second peak by increasing the average and the standard deviation of the lag by a considerable amount. This happens when the lag of a sample in the second peak includes a significant number of samples of the first peak.

The second parameter is the scale factor used in the calculation of the threshold. In the z-score algorithm, a higher scale factor requires peaks in the signal to have a larger gradient in order to be detected, since they have to be more standard deviations away from the moving average. This means that small peaks due to noise or multi-path will have a larger chance to be ignored, at the cost of possibly missing peaks corresponding to a target. The scale factor will not only depend on the pulse integration index (as explained in Chapter 4), but also on the characteristics of the room, such as for example the number of objects in the room, and the type of material of those objects. Therefore, the scale factor cannot be determined universally, but has to be adapted to the environment.

### Performance

The result of applying the z-score algorithm to the example measurement of Fig. 5.1 is shown in Fig. 5.2. In this measurement, a lag of 80 samples and a scale factor of 7.6 is used, which was found to approximately give the optimal result in this situation. Although the path followed by the target is clearly visible, there are a significant amount of erroneous detections visible in the graph that could not be removed without also removing a large part of the correct detections.

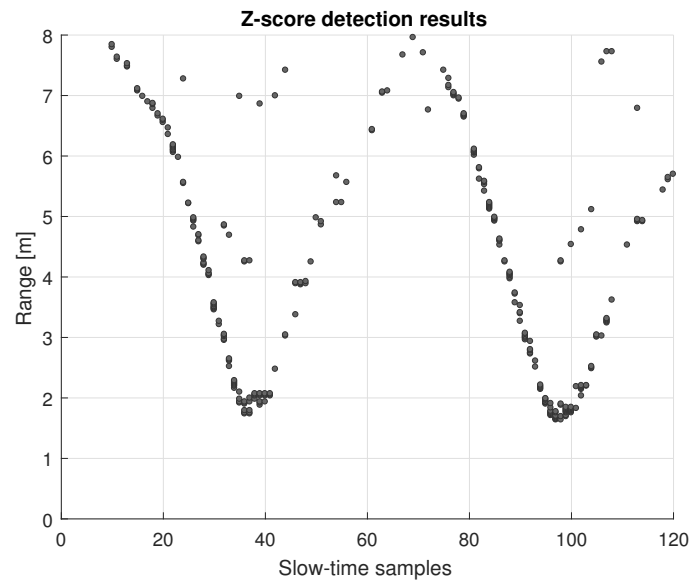


Fig. 5.2: Result of applying the z-score algorithm to the test measurement, with a scale factor of 7.6 and a lag of 80 samples.

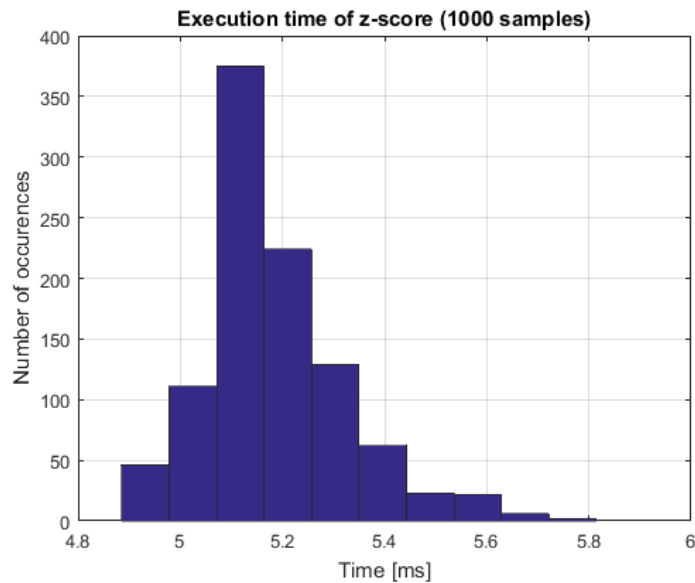


Fig. 5.3: Execution time of the z-score algorithm per radar, measured over 1000 executions.

The average execution time of the z-score algorithm is calculated by repeating the detection process 1000 times. The result is shown in Fig. 5.3. The average execution time is 5.18 ms. This means that for a system of four radars, the execution time of the algorithm by itself already exceeds 20 ms, which can possibly limit the refresh rate of the system and have a negative effect on the performance in real-time applications.

## 5.2 Range Compensated Average Threshold

Instead of focusing on the standard deviation of previous samples, which can be very computationally expensive, it may be beneficial to simplify the detection algorithm by purely focusing on the average of the signal.

### Algorithm Process

The simplest detection method that can be applied is to take the average of all the samples in the signal, followed by a comparison of each sample in the signal to a threshold. The threshold could simply be a constant scale factor multiplied by the signal average. However, a constant scale factor would result in a smaller probability of detection further away from the radar as the signal power disperses. To account for this, the scale factor is made inversely proportional to the distance from the radar, such that the threshold decreases as the distance from the radar increases. While this can potentially increase the amount of erroneous detections further away from the radar, the amount of correct detections increases as well. Therefore, a trade-off is made by selecting an optimal proportionality. The threshold  $\alpha$  for the RCAT algorithm is shown mathematically in Eq. 5.4.

$$\alpha = c \cdot \mu \cdot r^y \quad (5.4)$$

Here,  $c$  is the scale factor,  $\mu$  is the average of the signal,  $r$  is the distance from the radar and  $y$  is the proportionality coefficient.

### Performance

The result of applying the RCAT algorithm to the test measurement of Fig. 5.1 is shown in Fig. 5.4. From this graph, it is clear that no incorrect detections are made. Closer examination reveals that there are no missed detections in the path, although some slow-time samples contain fewer detections. Many detections are found in the vicinity of the path of the target, corresponding to a broad peak width of the target.

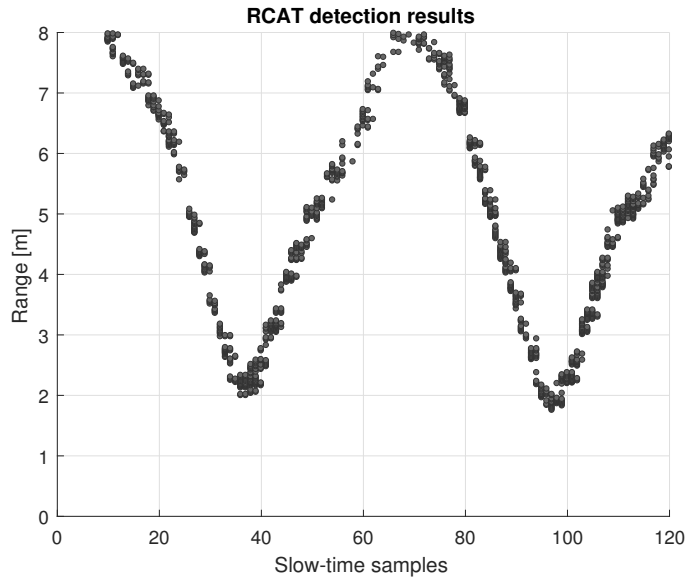


Fig. 5.4: Result of applying the RCAT algorithm to the test measurement, with a proportionality coefficient of 0.5 and a scale factor of 13500.

By applying the RCAT algorithm 1000 times to the test measurement, the average execution time can be estimated. The execution time measurement is shown in Fig. 5.5, and the average execution time per radar is 2.93 ms. For four radars, the execution time will be approximately 11.72 ms.

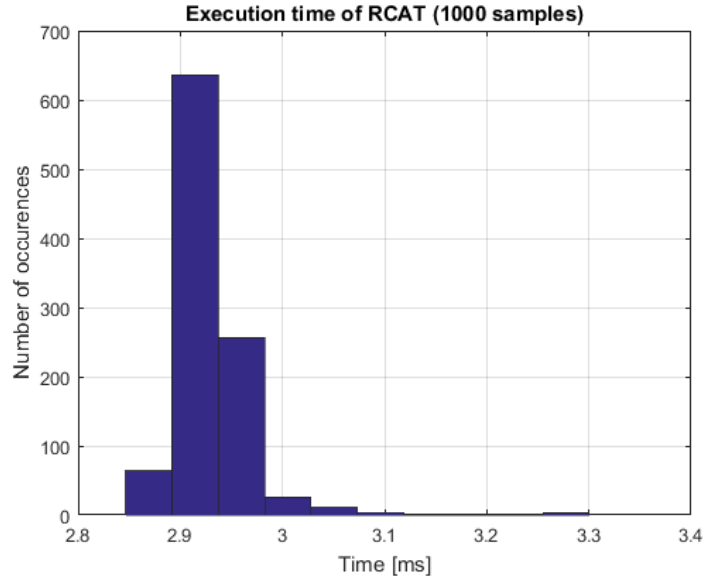


Fig. 5.5: Execution time of the RCAT algorithm per radar, measured over 1000 executions.

By comparing Fig. 5.2 and Fig. 5.4, it is clear that the detection accuracy of the RCAT algorithm is higher than that of the z-score algorithm. Considering the fact that the execution time of the RCAT algorithm is almost half of the execution time for z-score, it can be concluded that the RCAT algorithm performs better in both detection accuracy and execution time compared to the z-score algorithm.

It is important to note that, although the detection accuracy and the speed of the algorithm seems to be excellent in this test measurement, this algorithm is not very robust, because the average of the entire signal is taken, which can vary significantly depending on the number of moving targets in range of the radars. As a consequence, the scale factor will not only be dependent on the room characteristics and the pulse integration index, but also on the number of targets in range, which is often unknown or unpredictable in many applications. With more (moving) targets, the average of the signal rises, requiring a lower scale factor in order to have the same detection accuracy compared to a situation with less targets. In Fig. 5.4, the detection accuracy is extraordinarily high, but only because the scale factor was optimised afterwards. Changing the scale factor based on the estimation of the number of targets is not feasible nor reliable in real-time applications. Therefore, in Section 5.3, two algorithms are proposed that use local averages to determine whether a target is present or not, instead of using the average of the entire signal. While similar to the RCAT algorithm, using local averages will significantly improve the robustness of the detection.

### 5.3 Constant False Alarm Rate

The constant false alarm rate (CFAR) algorithm is commonly used in radar signal processing applications. [24] [25] In this section, two different types of CFAR algorithms are considered, namely the cell averaging (CA-CFAR) and least-of (LO-CFAR) variant. The main difference with the algorithm described in Section 5.2 is that instead of taking the average of the entire signal, as done in the previous algorithm, the signal is divided into cells of equal size, and local averages are used to determine target presence. The division of the signal in cells is graphically shown in Fig. 5.6.

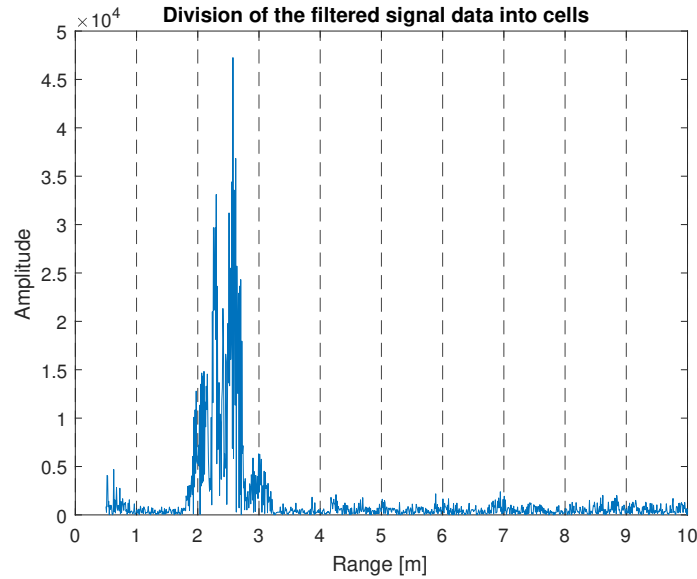


Fig. 5.6: Example of the division of the signal in several range-bins.

### 5.3.1 Cell Averaging Constant False Alarm Rate

As described above, the CA-CFAR algorithm starts with the division of the signal data into cells. A schematic representation of the algorithm is shown in Fig. 5.7.

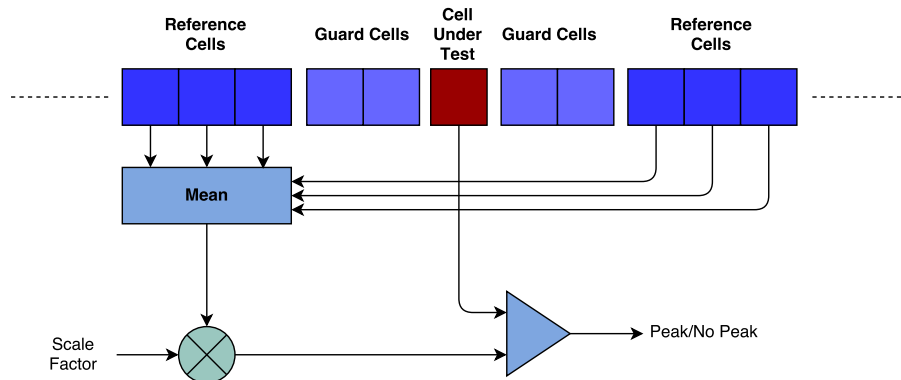


Fig. 5.7: Schematic representation of the CA-CFAR algorithm.

#### Algorithm Process

The schematic in Fig. 5.7 shows the process of the algorithm. A test cell is taken, which is called the cell under test (CUT). The algorithm tries to determine whether the CUT contains a peak or not. In order to achieve this, the mean value of the reference cells surrounding the CUT is calculated, such that an estimate of the noise can be made. However, in order to avoid using a cell which also contains part of the actual peak, guard cells are placed around the CUT, which are not used to calculate the average of the reference cells. The average of these reference cells are then scaled by a scaling factor in order to obtain the threshold. If the average of the CUT is larger than the threshold, a detection is made on the position of the CUT. Each cell of one data signal can be analysed in such a way by using a moving frame and performing the algorithm on each cell. The frame is symmetrical, which means that an equal number of guard cells and reference cells are used on each side of the CUT.

### Parameters

The parameters of the CA-CFAR algorithm are summarised in Table II.

Table II: Parameters of the CA-CFAR algorithm.

Parameter	Description
spb	The amount of samples in one cell
gc	The amount of guard cells (on one side)
N	The amount of reference cells (on one side)
scale	The scale factor for peak detection

By changing the number of samples in a cell, the algorithm can be made faster at the expense of a reduced resolution. Aside from the lower execution time with larger cell sizes, error rejection can be increased by having larger cell sizes. With more samples per cell, peaks with a relatively small width compared to the cell width can effectively be ignored in this algorithm. These peaks can correspond to noisy behaviour and generally do not come from a human target for small cell sizes, since the size of the target causes many reflections from different body parts. In order to test the detection algorithm with the full resolution of the radar, one sample per cell will be used.

The number of guard cells surrounding the CUT should be chosen based on an average peak width of targets. This way, it is possible to avoid part of the target reflection in the average of the surrounding noise, which could lead to a missing detection. From Fig. 5.6, it can be seen that the peak is about 0.9 m wide. Since the spatial resolution of the radar is 0.92 cm, there should be approximately 50 guard samples on each side.

The number of reference cells chosen determines over how many cells the average is taken. This should be high enough to calculate a reasonable noise average, but low enough to exclude a peak caused by the reflection of another target or by multi-path. This trade-off is very dependent on the situation. In the available test rooms for this project, 50 reference cells on each side suffices.

The scale factor is chosen based on the desired probability for a false alarm. Obviously, this error probability is desired to be zero. However, the probability of false alarm also determines the probability of detection, which means that decreasing the probability for false alarm will effectively decrease the number of correct detections made, reducing the performance of the algorithm. Therefore, a trade-off must be made, where a certain amount of false detections will have to be accepted in order to have an optimal algorithm. The scale factor is mathematically shown in Eq.5.5:.

$$\alpha = N \cdot \left( P_n^{-1/N} - 1 \right) \quad (5.5)$$

Here,  $\alpha$  is the scale factor,  $N$  is the amount of reference cells, and  $P_n$  is the probability of false alarm. By setting a constant false alarm, the ratio of correct and false detections can be set.

### Performance

The result of applying the CA-CFAR algorithm to the test measurement is shown in Fig. 5.8. The probability of false alarm has been set to 1.5%, which was necessary to detect the target at larger distances from the radar. Of the 1631 detections that were made, 29 were at an incorrect distance, resulting in a false alarm rate of 1.7%, which is close to the probability of false alarm that was initially set. Fig. 5.8 is a result of the trade-off made in order to detect the target by allowing a certain percentage of the detections to be incorrect. Since the CA-CFAR algorithm relies on local averages by using nearby samples to determine the noise level, this algorithm is more robust than the RCAT algorithm, discussed in Section 5.2.

The average execution time is determined from the average of 1000 executions of the algorithm. The result of this measurement is shown in Fig. 5.9, and the average execution time is 1.47 ms per radar, which

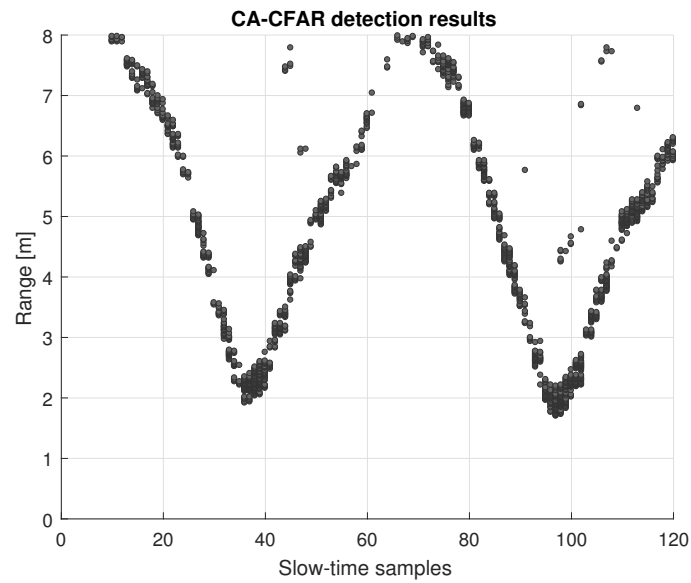


Fig. 5.8: Result of applying the CA-CFAR algorithm to the test measurement, with one sample per cell, 50 reference cells, 50 guard cells and a probability of false alarm of 1.5%.

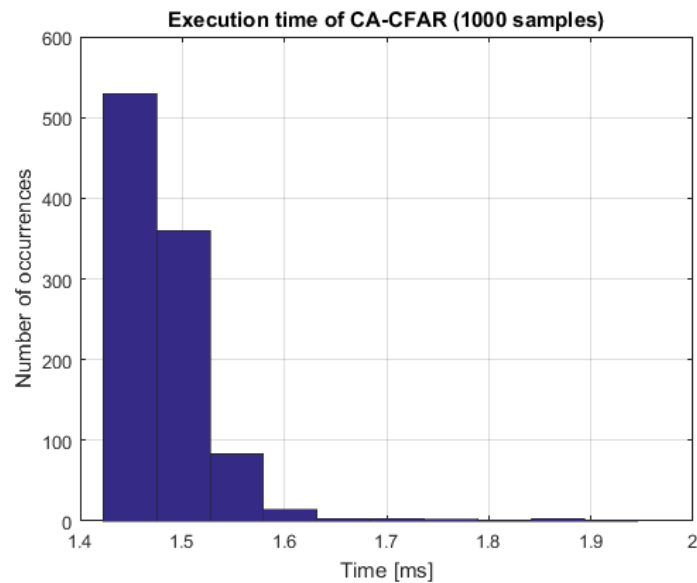


Fig. 5.9: Execution time of the CA-CFAR algorithm per radar, measured over 1000 executions.

amounts to 5.92 ms for all four radars. This algorithm is significantly faster than the z-score and the RCAT algorithm, described in the previous sections.

### 5.3.2 Least-Of Constant False Alarm Rate

A similar, alternative algorithm to CA-CFAR is the least-of constant false alarm rate (LO-CFAR). A schematic representation of this algorithm is shown in Fig. 5.10.

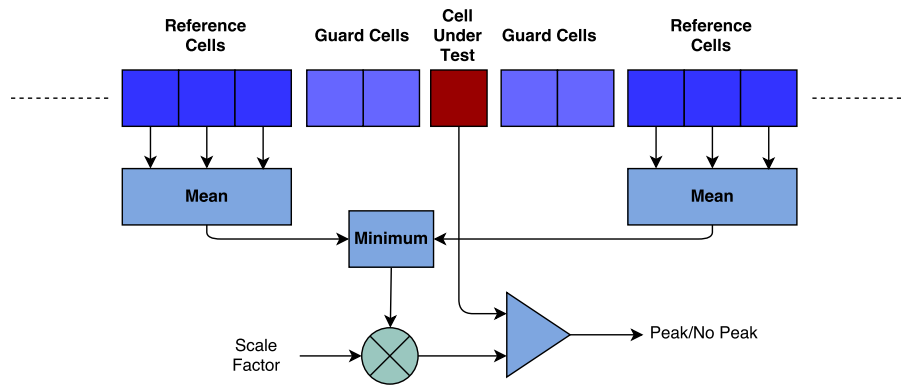


Fig. 5.10: Schematic representation of the LO-CFAR algorithm.

### Algorithm Process

Similar to the process described in Section 5.3.1, the fast-time signal is divided into cells, and the average of the reference cells close to the CUT is calculated. However, the main difference is in calculating the threshold value. Instead of using the average of the reference cells both left and right of the CUT to calculate the threshold value, only one side will be used. To determine which side will be used to calculate the threshold, the minimum of the two averages is determined. Taking the minimum will prevent comparing the CUT to the signal amplitude close to the CUT that is higher than the typical noise amplitude, caused by for example multi-path effects or background reflections. If the cells containing multi-path propagation would be considered, such as in CA-CFAR, there is a risk of missing a peak detection, because the average signal amplitude of the reference cells behind the peak is increased due to other reflections.

This algorithm has, by using the minimum of the two averages, an overall better performance in more cluttered areas, which is a common situation in indoor areas. In situations involving multiple persons, where two peaks caused by two different targets are potentially very close to each other, it is possible to detect both peaks while CFAR based solely on cell averaging might miss one or both of the peaks. Both CA-CFAR and LO-CFAR have the same algorithm parameters, which are described in Section 5.3.1. Compared to CA-CFAR, the increase in computational complexity is negligible, as the only difference is that a minimum value needs to be determined.

### Performance

The result of applying the LO-CFAR algorithm to the test measurement is shown in Fig. 5.11. The probability of false alarm is set to 1%. Compared to the result of the CA-CFAR algorithm, shown in Fig. 5.8, the LO-CFAR algorithm has more detections around the target path, and a similar amount of false detections. Of the 3257 detections that were made, only 27 were incorrect, resulting in a false alarm rate of 0.8%. The average execution time for 1000 tests is shown in Fig. 5.12, with an average execution time of 1.53 ms per radar, which is not significantly more than the execution time of the CA-CFAR algorithm of 1.47 ms, while being faster than the z-score and RCAT algorithm.

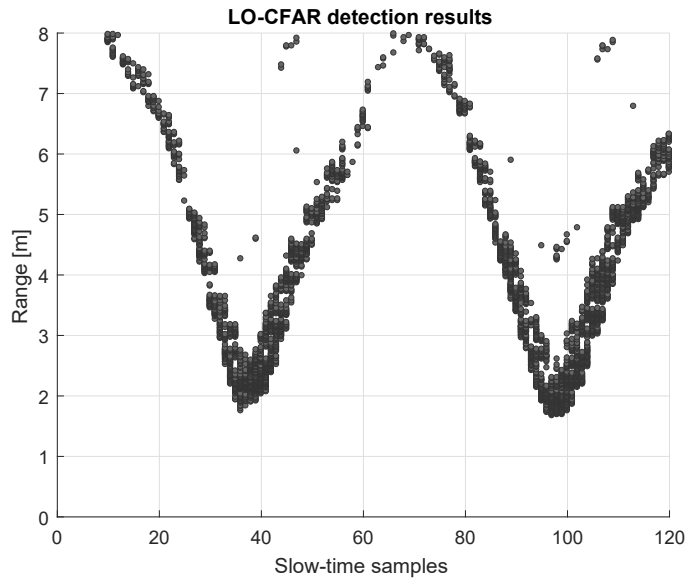


Fig. 5.11: Result of applying the LO-CFAR algorithm to the test measurement, with 1 sample per cell, 50 reference cells, 50 guard cells and a probability of false alarm of 1%.

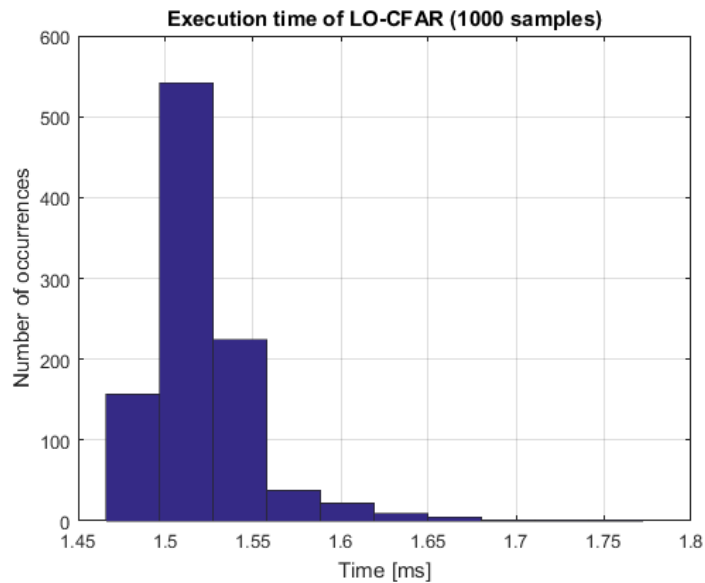


Fig. 5.12: Execution time of the LO-CFAR algorithm per radar, measured over 1000 executions.

## 5.4 Detection Clustering

Since the algorithms above apply a test condition to each sample (or cell) in the signal, it is possible that there are multiple detections close to each other, each belonging to the same detected person. In order to interpret multiple detections as coming from a single target, an algorithm is developed to cluster detections and replace a bulk of detections by one single distance at the average position of the detections.

The simplest method to cluster several detections into one (possible) target is to look at the detection density in the fast-time signal. For each sample in fast-time, the local density of detections in a frame of

width  $w$  is considered. This is simple to implement by applying a convolution of a rectangular pulse to the data sequence, and truncating the result to the length of the original signal. The convolution is shown mathematically in Eq. 5.6.

$$\rho[n] = x[n] * (u[n + \frac{w}{2}] - u[n - \frac{w}{2}]) \quad (5.6)$$

Here,  $\rho[n]$  is the detection density,  $x[n]$  is the detection sequence of the fast-time signal and  $u[n]$  is the unit step function. The sequence  $\rho[n]$  can now be used to determine positions of possible targets in the fast-time scan by evaluating peaks in the detection density. This is done using the MATLAB function *findpeaks*. Within this function, it is possible to set the number of peaks to be detected, the minimal distance between peaks to exclude local peaks in the vicinity of a large peak, and the minimal height of a peak, corresponding to the minimal amount of detections nearby.

An example of a detection density can be made based on the signal in Fig. 5.6. Using the LO-CFAR algorithm described in Section 5.3.1, the LO-CFAR algorithm is applied to the test measurement of Fig. 5.6 such that an example detection density plot can be created. The width of the rectangular pulse is chosen to be 50 samples. The result is shown in Fig. 5.13. From this graph, it is clear that there is one distinctive peak in the signal, corresponding to one target, which will be placed on the position with the highest detection density. The figure also shows the importance of excluding local maxima in the detection density.

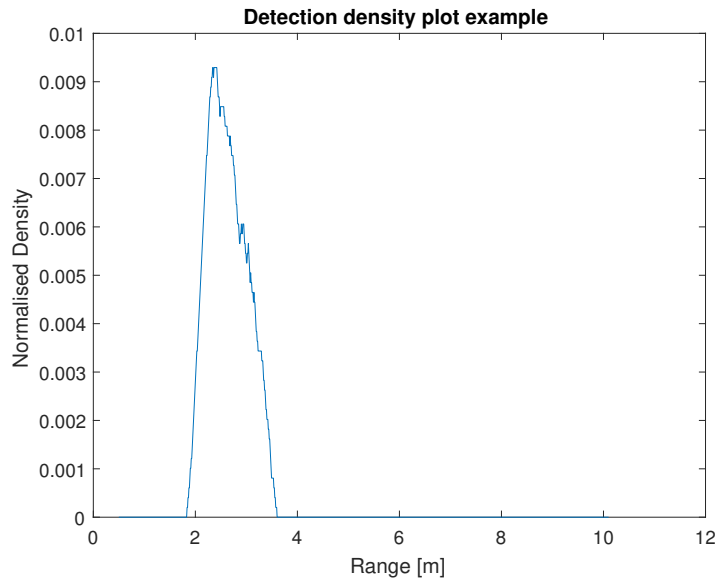


Fig. 5.13: Detection density plot of the signal in Fig. 5.6.

The detection clustering algorithm can now be applied to the example measurement. By using the detection results of the LO-CFAR algorithm shown in Fig. 5.11, the target positions in the example measurement are determined. The result of applying the detection clustering algorithm is shown in Fig. 5.14. The average execution time for 1000 executions is shown in Fig. 5.15. Over these 1000 executions, the average execution time is approximately 5.26 ms.

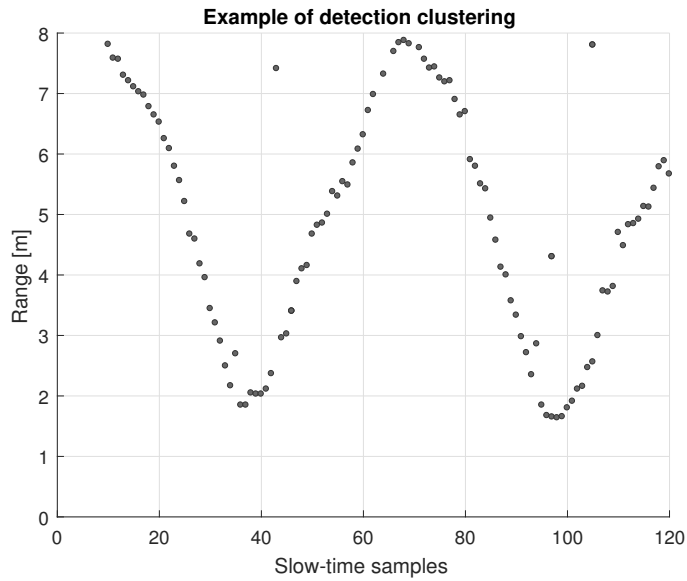


Fig. 5.14: Target clustering of the detection results from the LO-CFAR algorithm applied to the example measurement.

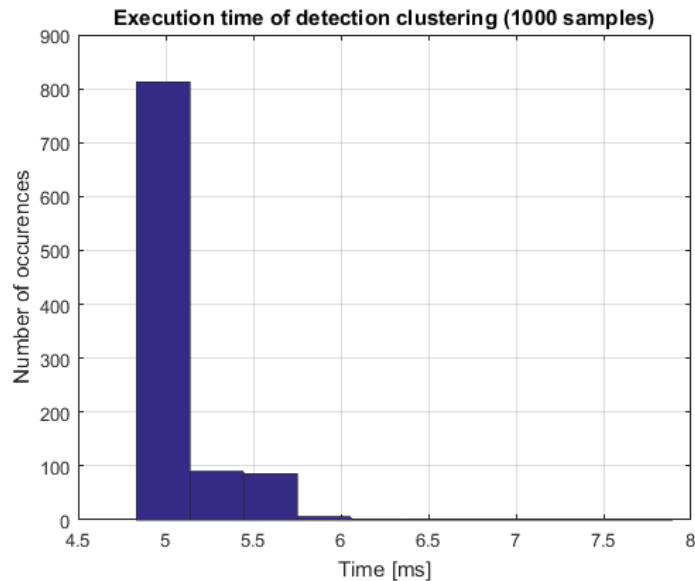


Fig. 5.15: Execution time of the detection clustering algorithm, measured over 1000 executions.

## 5.5 Discussion

The performance of each algorithm in the test measurement of Fig. 5.1 is summarised in Table III. The performance criteria include the detection accuracy, execution time and robustness of the algorithm. The detection accuracy is based on the number of false detections and missed correct detections. The execution time is simply the time required for the algorithm to complete, and the robustness is based on its versatility with respect to multiple targets and different room characteristics. The scores for each algorithm in Table III are relative to each other.

It can be concluded that the z-score algorithm has a much lower performance than the other algorithms. The RCAT algorithm has an excellent detection accuracy and a decent execution time, but under-performs

Table III: Algorithm performance in the test measurement based on detection accuracy, execution time and robustness.

Algorithm	Detection Accuracy	Execution Time	Robustness
<b>z-score</b>	-	--	+
<b>RCAT</b>	++	+/-	--
<b>CA-CFAR</b>	+	++	+
<b>LO-CFAR</b>	+	+	++

when it comes to versatility, since the scale factor is dependent on the average of the entire signal, which may change depending on the number of targets present. This is undesirable, because in most practical situations, it is unknown how many targets are present within the range of a radar. Both the CA-CFAR algorithm and the LO-CFAR algorithm do have this versatility, by using local averages instead of a global signal average. The trade-off for this versatility is that the detection accuracy goes down. However, as long as the ratio of correct and incorrect detections remains low, by setting a relatively low probability of false alarm, this will not be a problem for tracking of the target(s), especially when only one or two radars make an error at this specific location. As long as the erroneous detections are uncommon, the tracking module can reject these detections. [1]

When comparing the least-of CFAR to the cell-averaging CFAR, the only significant difference is that the LO-CFAR algorithm misses fewer detections in situations where the signal behind the target becomes noisy due to multi-path reflections. This makes the LO-CFAR algorithm slightly more robust compared to CA-CFAR, especially when two targets are close to each other, causing the local average on one side to go up. The difference in execution time is only about 0.05 - 0.1 ms per radar, which has a negligible effect on the refresh rate of the system. Therefore, the LO-CFAR algorithm has the ability to supply better multi-person detection results, making it the optimal detection algorithm in this application.



# Chapter 6

## Velocity Estimation

In order to satisfy all user requirements, not only the position of a target is desired, but the velocity of the target as well. By estimating the velocity of targets in addition to their location, the accuracy of a tracking system can be greatly improved. Therefore, it could prove to be useful to investigate the possibility of implementing velocity estimation in a real-time tracking application.

In this chapter, Range-Doppler processing is discussed. In Section 6.1, a description is given of the Doppler effect and its utilisation in Range-Doppler processing. Two-dimensional velocity estimation is explained in Section 6.2. Simulation results for Range-Doppler processing are shown in Section 6.3, and the limitations of Range-Doppler processing in real-time applications are discussed in Section 6.4. Other methods to determine the velocity of the target are further discussed in the tracking module of the system, discussed in [1].

### 6.1 Range-Doppler Processing

Range-Doppler is a processing technique often used in radar systems to determine the velocity of a target. [26] Due to the Doppler effect, any wave reflecting from a target moving towards or away from the transmitter will be shifted in frequency. In a technique called Range-Doppler radar processing, this shift in frequency is used to estimate the velocity of targets from the received radar signal. By taking the FFT in the time-direction of several slow-time measurements, a frequency spectrum is obtained for each fast-time sample. If there is a person walking towards or away from the radar at a certain distance, the spectrum will contain a frequency component which corresponds to the velocity of the person. This frequency can be converted into a velocity, which will be the radial velocity of the target with respect to the radar.

In its simplest form, the Doppler frequency shift is mathematically described by Eq. 6.1. [27]

$$f_D = \frac{c - v_r}{c + v_t} f_i \quad (6.1)$$

In this equation,  $v_r$  represents the radial velocity of the receiver with respect to the transmitter,  $v_t$  represents the radial velocity of the transmitter with respect to the receiver,  $c$  represents the propagation speed of the wave,  $f_D$  represents the Doppler shifted frequency, and  $f_i$  represents the incident wave frequency.

In the case of Range-Doppler with a radar system, the receiver and transmitter are both located at the radar, resulting in the Doppler effect occurring twice. At first, the radar is the transmitter, and the person can be considered as the 'receiver'. The Doppler shift occurs when the wave reflects off of the person. From here, the wave travels back to the radar, but this time, the person can be considered the 'transmitter', and the radar is the receiver, causing another Doppler shift by the same factor as in the first shift. The result of this double Doppler shift is shown in equation Eq. 6.2. In this equation,  $f_b$  is the change in frequency as a result of the Doppler effect, also called the beat frequency, and  $v$  is the target's radial velocity with

respect to the radar. In this equation, the assumption is made that the velocity of the target is much smaller than the speed of light, which is a reasonable assumption in person tracking applications.

$$f_b = \frac{2v}{c+v} f_i \approx \frac{2v}{c} f_i \quad (6.2)$$

The beat frequency can be estimated in the frequency spectrum, and converted to a physical velocity of the target using Eq. 6.3.

$$v = f_b \cdot \frac{c}{2f_i} \quad (6.3)$$

For UWB radars, there is no singular initial frequency but rather a frequency band with a width of several GHz. The relative width of this band, i.e. the bandwidth as a fraction of the centre frequency, is relevant to the Range-Doppler algorithm. Since beat frequency is linearly dependent on the initial wave frequency, the beat frequency will have the same relative bandwidth as the transmitted pulse. The formula for this relative bandwidth is seen in Eq. 6.4.

$$B_r = \frac{B}{f_c} = \frac{2.2 \text{ GHz}}{4.2 \text{ GHz}} \approx 0.52 \quad (6.4)$$

In this equation,  $B_r$  is the relative bandwidth,  $B$  is the absolute bandwidth, and  $f_c$  is the centre frequency. In the case of the P410 module, the bandwidth is 2.2 GHz and the centre frequency is 4.2 GHz, resulting in a relative bandwidth of approximately 0.52.

In the frequency spectrum of the radar data, peaks will appear at the beat frequency corresponding to the radial velocity of the target with respect to the radar. To estimate a target's velocity from this spectrum, the one-dimensional CFAR algorithm, discussed in Section 5.3, is applied to the frequency spectrum of each range bin where a target was detected. The peak in the received frequency band most likely corresponds to the peak in the transmitting frequency band. Because of this, the peak frequency of the transmitted signal's frequency band is used to convert the received peak frequency to a target velocity in Eq. 6.3. Since the peak of the transmitted signal's frequency band is at its centre frequency, that's the frequency to be used as  $f_i$  in Eq. 6.3 to convert a peak frequency to a target's velocity.

The velocity estimation that is obtained from Range-Doppler processing can be utilised in the tracking module, as explained in [1]. If the velocity of the target is available to the tracking algorithm, the incorrect detections can be more accurately and more reliably rejected, and adds the possibility of replacing incorrect detections with estimations of target positions. Velocity measurements can also be used to resolve any tracking conflicts caused by two or more targets crossing paths, instead of solely relying on positions.

## 6.2 2-D Velocity Estimation

Since Doppler shift only depends on the radial velocity of a target with respect to the radar, more radars are required to estimate the true velocity of a target. The two- or three-dimensional velocity of the target cannot be measured through the Range-Doppler technique with only one radar device. Instead, the radial velocities with respect to multiple radars, along with the known location of the target, are used together to estimate the two-dimensional velocity of the target.

In Appendix B, an explanation is given as to how the information from Range-Doppler processing and the target location is used to estimate the two-dimensional velocity of the target.

## 6.3 Simulation Results

To test the algorithm, Range-Doppler processing is applied to a simulated dataset. This dataset was made by constructing a pulse with the same centre frequency, bandwidth and sample frequency as the pulse

generated by the real radar device, and shifting it in the range dimension. This dataset is shown in Fig. 6.1. The red line in this image indicates the current scan position in time, at which the Range-Doppler algorithm is performed. This image shows a simulated target at a distance of approximately 3.5 m from the radar. The Range-Doppler image at this time-instant is shown in Fig. 6.2. A clear peak can be seen at the position of the simulated target, with a velocity of 1 m/s with respect to the radar.

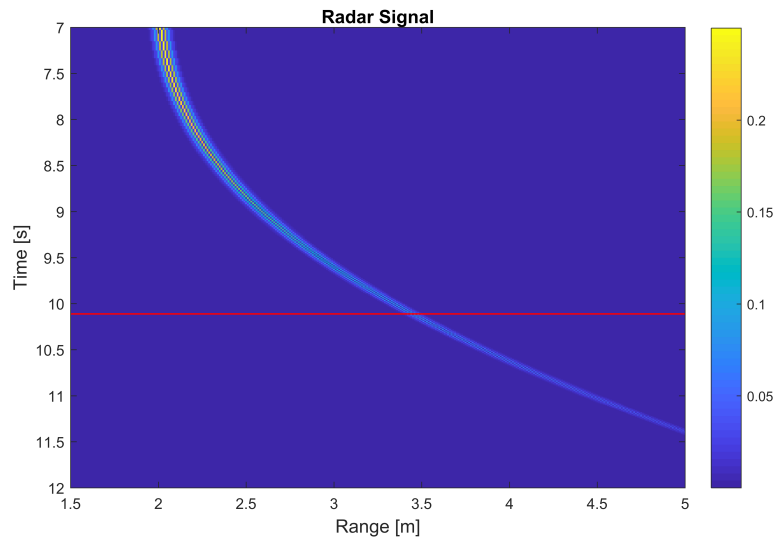


Fig. 6.1: Simulated dataset on which the Range-Doppler algorithm will be applied. Shown is the time-domain radar signal as received after background rejection. The red line indicates the time at which the Range-Doppler algorithm is performed.

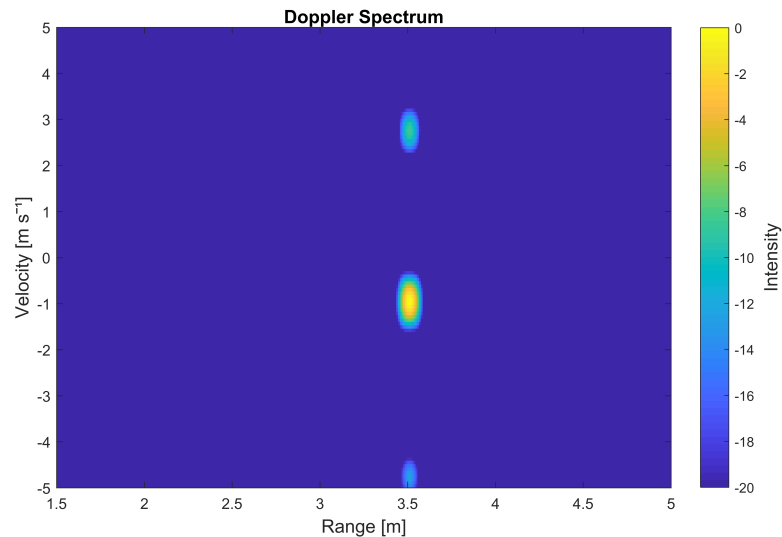


Fig. 6.2: Doppler spectrum of the data shown in Fig. 6.1 at the indicated slow-time measurement.

Some sidelobes can be seen at clear integer multiples of the centre frequency, which is to be expected from a windowed gaussian pulse. The sidelobes can be filtered out either by the peak-detection algorithm, or by a tracking algorithm.

## 6.4 Limitations

Range-Doppler processing uses a Fourier transform in the slow-time direction to determine the frequency spectrum for each fast-time range. The maximum velocity that can be detected thus depends on the sample frequency in slow-time. Any velocity greater than half of the sample frequency will be incorrectly represented in the frequency domain due to aliasing. This puts a limitation on the maximum velocity that targets in the area are allowed to have such that Range-Doppler processing works correctly.

According to the Nyquist criterion, the maximum beat frequency must be smaller than half the sampling frequency to prevent aliasing. Equation 6.5 shows the constraint on the maximum velocity that can be coherently determined with a certain sample frequency.

$$v < \frac{cf_s}{4f_i} \quad (6.5)$$

Here,  $v$  is the velocity of the target,  $f_b$  is the beat frequency due to the Doppler shift,  $f_i$  is the centre frequency of the radar,  $c$  is the speed of light and  $f_s$  is the slow-time sample frequency. Using the P410 module's centre frequency of 4.2 GHz and a pulse slow-time sample frequency of approximately 11 Hz, based on a PII of 11, a maximum coherently measurable target velocity of approximately  $0.20 \text{ m s}^{-1}$  is obtained.

In order to meet the user requirements described in Section 2.1, the system must be able to detect target velocities of up to  $2 \text{ m s}^{-1}$ . According to Eq. 6.5, the minimum sampling frequency required to correctly detect these velocities is 115 Hz. Since the maximum sample frequency with the PulsON radar system is 17.3 Hz, the user requirement cannot be met with range-Doppler processing. Therefore, a different velocity estimation method is required, which is discussed in the tracking module of the system. [1]

## 6.5 Improvements

Various filtering algorithms can be used to make the peaks in the velocity-range spectrum easier to detect. For instance, the frequency spectrum could be deconvoluted with the spectrum of a known peak. This would result in sharper peaks that are easier to detect.

Instead of using a one-dimensional peak detection algorithm at several range, a two-dimensional peak detection algorithm could be applied to the entire two-dimensional spectrum. This would result in both velocity and location data being detected. Additionally, this would possibly result in more accurate peak detections since side-lobes would not be as significant.

A range migration algorithm could be applied to the radar data, such that the Fourier transform is taken over multiple samples in the movement direction of the target, rather than at static ranges. This is a concept called range migration, and is discussed further in [28]. This would result in a more coherent spectrum of the target, possibly improving Doppler accuracy.

# Chapter 7

## Results

In this chapter, the results of several tests are shown. In order to demonstrate the capability of the detection system, an open area as well as a cluttered area is used to detect both a single target and multiple (two) targets. The cluttered area used for testing is a small, 5x8 metre room with many objects of different materials, including highly reflective metal objects. This will ensure that many multi-path reflections will be present. The open area and its immediate surroundings contain no large objects in the vicinity of the radars. In Section 7.1 the test results for a single target in an open and a cluttered area are presented and discussed. The results for two targets are discussed in Section 7.2. Through wall measurements have been done, and will be discussed in Section 7.3. The detection algorithm used to obtain the results is the LO-CFAR algorithm described in Section 5.3.2, combined with the detection clustering algorithm described in Section 5.4. The detections and target ranges that are obtained from measurements can be used to localise and track the target, as discussed in [1].

### 7.1 Single Person Detection

The detection of a single person is a relatively simple problem. Based on measurements of the room characteristics, such as the room size and the effect of multi-path reflections from targets in the room, the probability of false alarm can be set to optimise the detection accuracy of the algorithm. The path walked by a single person during the measurement is shown graphically in Fig. 7.1. The measurements are taken from the perspective of radar 1, and the nearest point visible in each graph is marked by S.

#### 7.1.1 Open Area

The radar range image of a single person in an open area is given in Fig. 7.2. As seen from this figure, in the open area the person is clearly visible, and the multi-path reflections are minimal. There are no large objects in range of the radar that would cause significant reflections, making the detection trivial. Because of the open environment, the optimal probability of false alarm can be set to a low value without losing too many correct detections.

The detections as a result from applying the LO-CFAR algorithm to the filtered signal with a probability of false alarm of  $P_{fa} = 10^{-3}$  are shown in Fig. 7.3a. From this figure, it is clear that the target has successfully been detected, and that only a few erroneous detections are made at positions where the noise and multi-path was slightly too high. The final result after detection clustering is shown in Fig. 7.3b. Except for a few incorrect detections, the target has been correctly detected across its entire path. The incorrect detections and target positions are rare and sufficiently spaced, such that the tracking module can effectively filter these positions instead of creating a new target path. Therefore, the incorrect target detections are acceptable, and do not have to be further accounted for by the detection system. Aside from the incorrect detections, 100% of the path of the target has been detected in this measurement, which meets the requirement posed in Section 2.4.



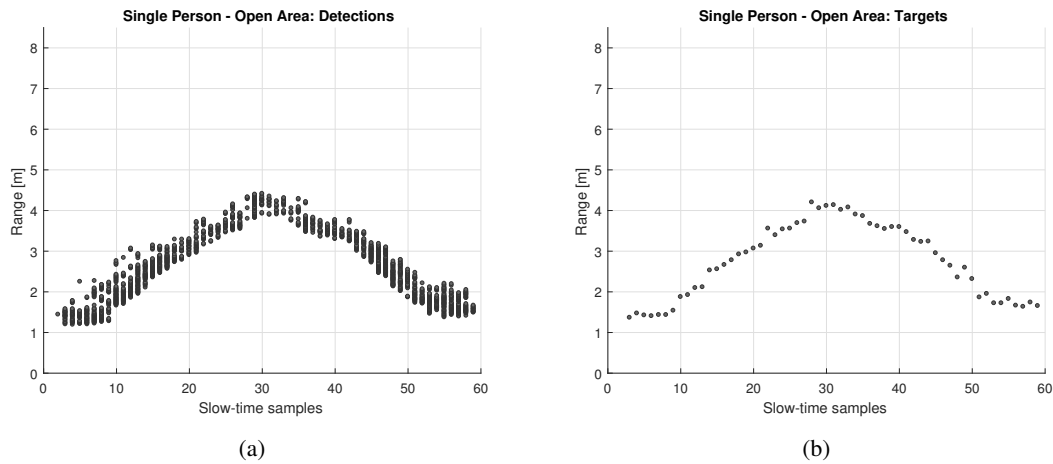


Fig. 7.3: The results of applying (a) the LO-CFAR algorithm and (b) the detection clustering algorithm to the radar range image of Fig. 7.2.

pattern of these higher sample amplitudes vaguely resemble the movement of the target, suggesting that the cause of the higher amplitudes is indeed multi-path reflections. Other than the increase in multi-path effects, the situation is fairly similar to the measurement in Section 7.1.1.

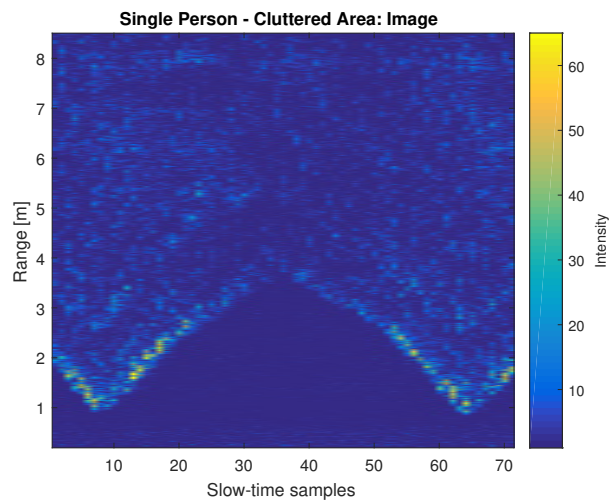


Fig. 7.4: Radar range image of a single person in a cluttered area walking towards and away from the radar.

The resulting detections and the target positions are shown in Fig. 7.5a and Fig. 7.5b respectively. The probability of false alarm is set to  $P_{fa} = 10^{-2}$ , which is necessary to reject many of the incorrect detections without losing too many correct detections. There seem to be more incorrect detections compared to the single person measurement in the open area, described in Section 7.1.1, and the number of correct detections has decreased. However, the decrease in correct detections is not significant, because the target is still clearly observable by the radar. Figure 7.5b shows the detected path of the target. Approximately 96% of the target path has been detected, which is in accordance with the technical specifications. However, a secondary path parallel to the target path seems to arise, which is most likely caused by multi-path reflections. Because these erroneous target positions resemble a legitimate path, this could lead to problems in the tracking module, as it might be recognised as a second target.

The detections are again compared to the distances expected from Fig. 7.1. The minimum range detected is 1.21 m on both sides, 20 cm from the expected distance of 1.41 m. The maximum distance is 3.95 m, 29 cm from the expected location.

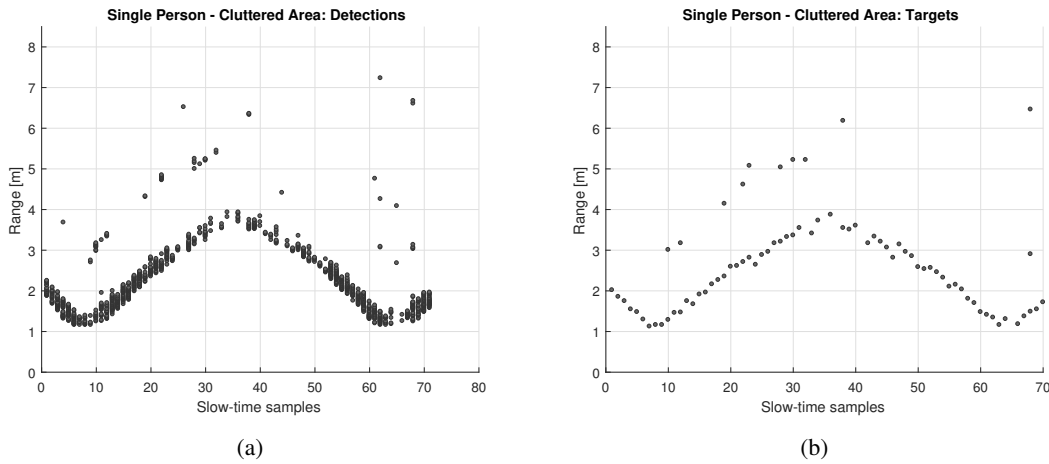


Fig. 7.5: The results of applying (a) the LO-CFAR algorithm and (b) the detection clustering algorithm to the radar range image of Fig. 7.4.

It is possible to increase the minimum detection density such that this path is rejected before it is used by the tracking module. The result of increasing the minimum detection density to four detections in a frame width of 50 samples is shown in Fig. 7.6. The multi-path positions are now almost completely rejected, but at the cost of the correct path of the target. However, it may be beneficial to make this trade-off if the loss of correct target positions is kept small. In Fig. 7.6, approximately 72% of the path of the target is successfully detected, and only one erroneous detection is made. Although the detection accuracy is lower compared to the result shown in in Fig. 7.5b, the number of incorrect detections has been reduced significantly, while still meeting the requirements of the system.

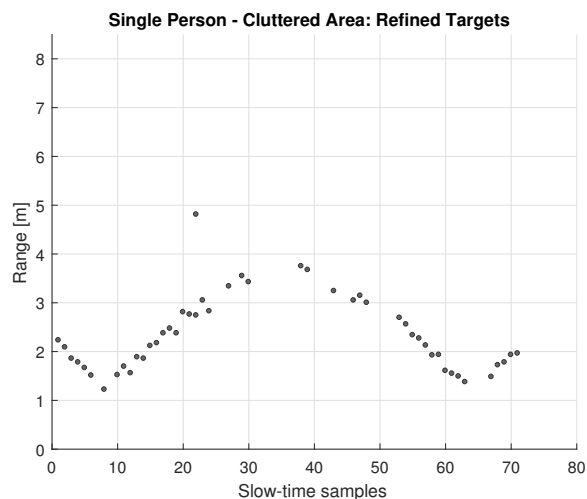


Fig. 7.6: The results of applying the detection clustering algorithm to the detections of Fig. 7.5a with a minimum detection density of four.

## 7.2 Multiple Person Detection

When instead of one target, multiple targets are present in the area, the detection of these targets becomes a challenge. This is especially the case in cluttered areas, because one of the targets is possibly in the range of the multi-path reflections of the other target(s), increasing the difficulty of detection. In addition, there might be a reflection from one target to the other target, back to the radar, although the amplitude of this received reflection should be significantly lower if the target has a (relatively) low reflection coefficient. Summarised, multiple person detection introduces a lot of difficulties with detection. Multi-path reflections might be observed as a person, and additional targets could be missed due to the increased signal level due to multi-path reflections around the additional targets. In Section 7.2.1 and Section 7.2.2, an attempt is made to distinguish two targets in an area of 4x4 metres by applying the previously discussed LO-CFAR algorithm and detection clustering. The two targets will cross each other in a centre point in front of the radar; one target walks directly towards and away from the radar, while the motion of the other target is perpendicular to the motion of the first target. The path walked by the two persons is illustrated in Fig. 7.7. The two persons walk back and forth, crossing each other in twice in the centre of the area enclosed by the radars.

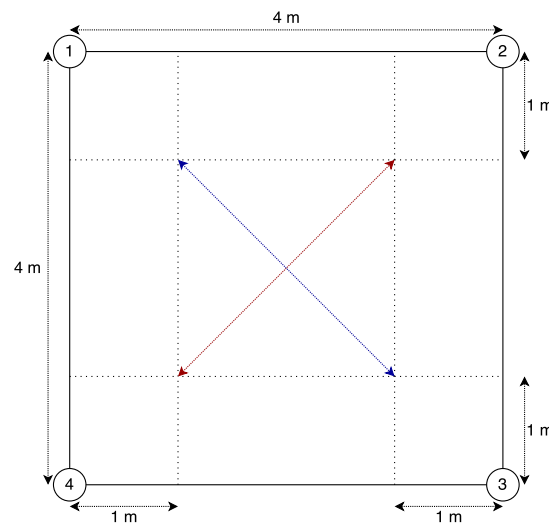


Fig. 7.7: Walking pattern for the multiple person measurements. The circles represent the radars, and the arrows represent the path walked by the targets.

### 7.2.1 Open Area

The radar range image of two persons moving in an open area is shown in Fig. 7.8. The two paths of the targets are clearly visible in the image, which is promising for the detection results. The multi-path effects seem to be low compared to the reflections coming directly from the target.

The resulting detections and the target positions are shown in Fig. 7.9a and Fig. 7.9b respectively. With a probability of false alarm of  $P_{fa} = 10^{-3}$ , similar to that of the open area measurement described in Section 7.1.1, no incorrect detections are found, and the two paths are clearly visible. However, when the persons cross, it becomes difficult to distinguish the two targets, since the reflections are at similar ranges. This can possibly cause issues for maintaining the track of the two targets, as the motion at the crossing point is ambiguous. It is unclear whether they cross paths, or simply meet at the centre and proceed to walk in a different direction. If target velocities can be estimated, and if the assumption can be made that this velocity does not change rapidly, then this issue could be resolved. If the position where the target paths cross is excluded from the calculation, then both targets show a detection accuracy of over 90%, with no further incorrect detections made.

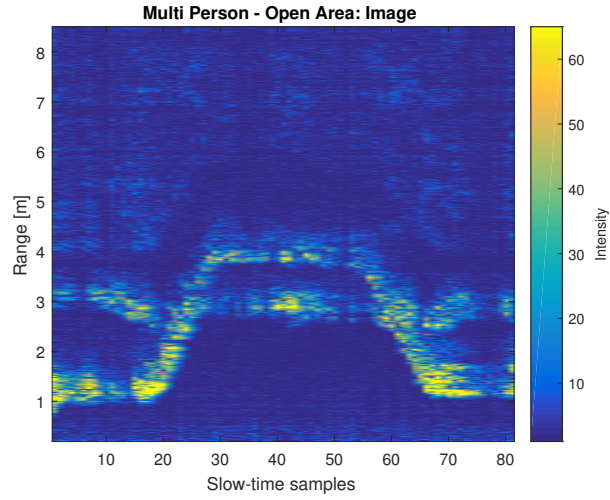


Fig. 7.8: Radar range image of two persons in an open area crossing paths perpendicularly twice.

The measurement is now compared to the distances expected from Fig. 7.7. The detections at the centre of the plot are expected to be at a distance of 3.16 and 4.24 m. The persons are detected at 2.95 and 4.07 m. This gives a discrepancy of 21 and 17 cm, respectively. The left and right side show the closer person at a distance of 1.42 m, only 1cm from the expected distance of 1.41 m.

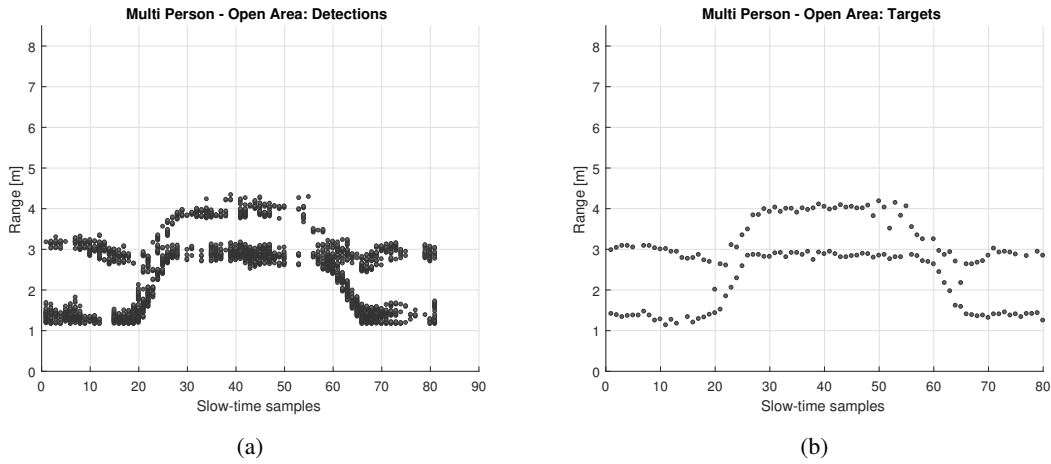


Fig. 7.9: The results of applying (a) the LO-CFAR algorithm and (b) the detection clustering algorithm to the radar range image of Fig. 7.8.

## 7.2.2 Cluttered Area

The range image for two persons in a cluttered area is shown in Fig. 7.10. In this measurement, it is very difficult to see the target furthest away from the radar because of the multi-path reflections caused by the closer target, essentially hiding the direct reflections from the further target.

The resulting detections and the target positions are shown in Fig. 7.9a and Fig. 7.9b respectively. The probability of false alarm is set to  $P_{fa} = 10^{-2}$ , in order to attempt to detect both targets. The only reliable section of the measurement is when the two persons are furthest away from each other, which is for slow-time samples 40 through 100. It is clear that the multi-path reflections are too significant for the detection system to successfully distinguish two targets and to reject incorrect detections.

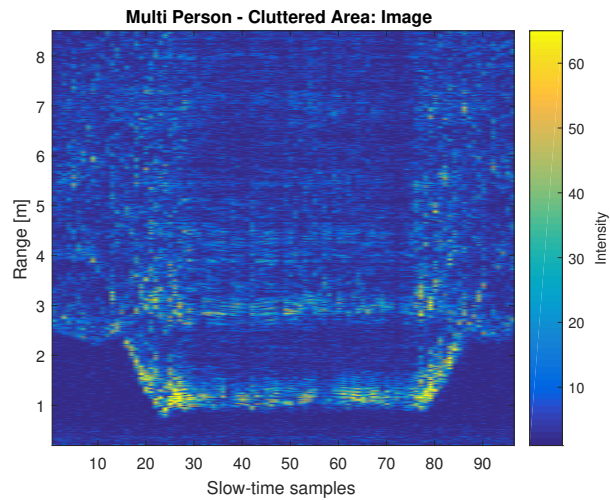


Fig. 7.10: Radar range image of two persons in a cluttered area, crossing paths perpendicularly twice and walking parallel to each other.

Unfortunately, a higher probability of false alarm only introduces more incorrect results instead of the path of the additional person. It is clear that the detection accuracy requirement has not been met, and that the system is not capable of detecting two persons in this particular room. Aside of the middle section of the measurement, it is not possible to determine a logical path of the person furthest away from the radar. Further increasing the PII gave similar results.

Comparing the measurement to the expectations shows that the centre of the measurement has a difference of 23 cm for the closer person and 32 cm for the person further away. The sides cannot be compared due to the lack of detections.

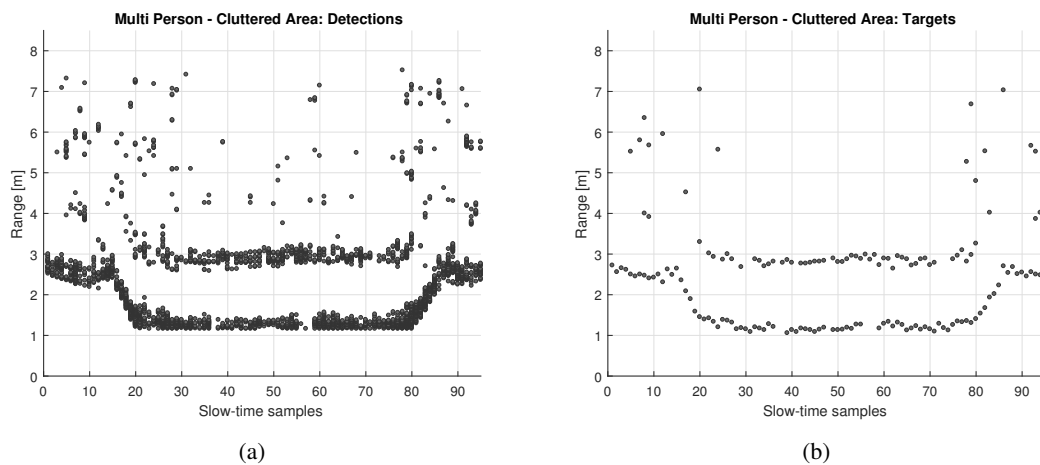


Fig. 7.11: The results of applying (a) the LO-CFAR algorithm and (b) the detection clustering algorithm to the radar range image of Fig. 7.10.

## 7.3 Through-wall Detection

If the tracking system is to be used in indoor applications, it is important that the radar signal has the ability to penetrate objects such as plants, tables and even walls. One of the advantages discussed in the

state-of-the-art analysis in Section 2.3 is that electromagnetic waves have the ability to penetrate objects. However, this does depend on the frequency of the wave, and the material that has to be penetrated. A metal plate, for example, has a very small penetration depth even for lower frequencies, and will block the wave almost completely, blocking the ability to sense any targets behind the metal. In this measurement, the ability to see through a concrete wall with a width of 20 cm is tested, in order to determine whether the user requirement for through-wall tracking can be met. The radar is placed behind the wall, and a single person on the opposite side of the wall walks by in a straight line. This is graphically shown in Fig. 7.12.

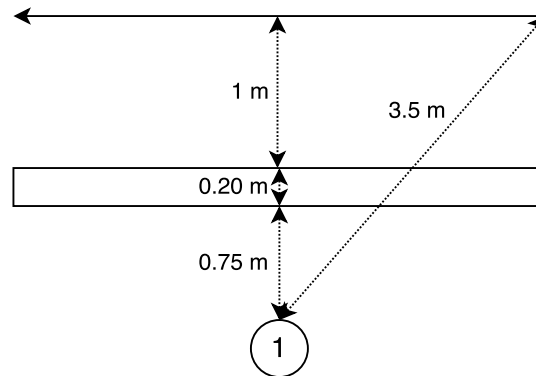


Fig. 7.12: Walking pattern for the through-wall measurement. The circle represents the radar, and the arrow represents the path walked by the target.

The radar range image of the through-wall detection measurement is shown in Fig. 7.13. A pulse integration index of 11 is used for this measurement. As seen in Fig. 7.13, the person is still clearly visible, even though the wave has to travel through the concrete wall twice. The maximum distance which gave reliable detection results was approximately 4 metres. Beyond this range, almost no detections are made at the position of the person. With higher pulse integration indexes, this range could be extended, at the cost of a reduced slow-time sample frequency, which can have major impacts on real-time applications.

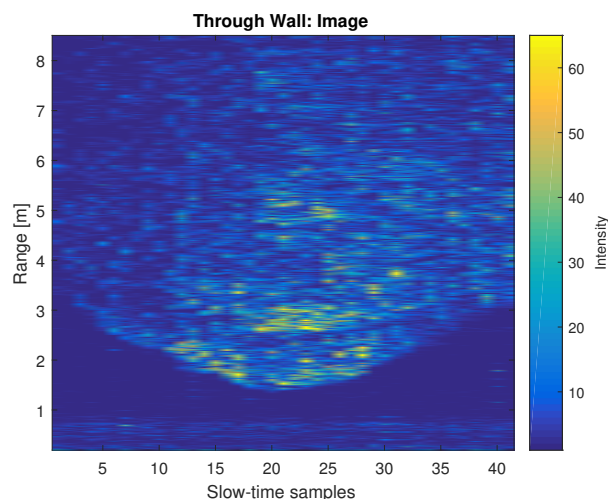


Fig. 7.13: Radar range image of a single person walking in a hallway, with the radar behind the wall.

The detections and target position are shown in Fig. 7.14a and Fig. 7.14b respectively. The probability of false alarm is set to  $10^{-2}$ . A notable erroneous detection is found behind the target in the middle of the measurement. This error is caused by the target walking in front of a metal radiator. The motion filter then causes a peak to arise at the position of the metal radiator. Other erroneous detections are most likely due

to random noise and clutter. Despite the few incorrect detections, through-wall target detection is working as expected. Over 90% of the path of the target is detected, and the three incorrect detections are spaced far enough to be rejected in the tracking system. The user requirement for non-line-of-sight detection has been met.

The expected minimum and maximum distance are 1.95 and 3.5 m, respectively. The measured distances are 1.67 and 3.3 m, as seen in Fig. 7.14b. This gives a discrepancy of 28 and 20 cm.

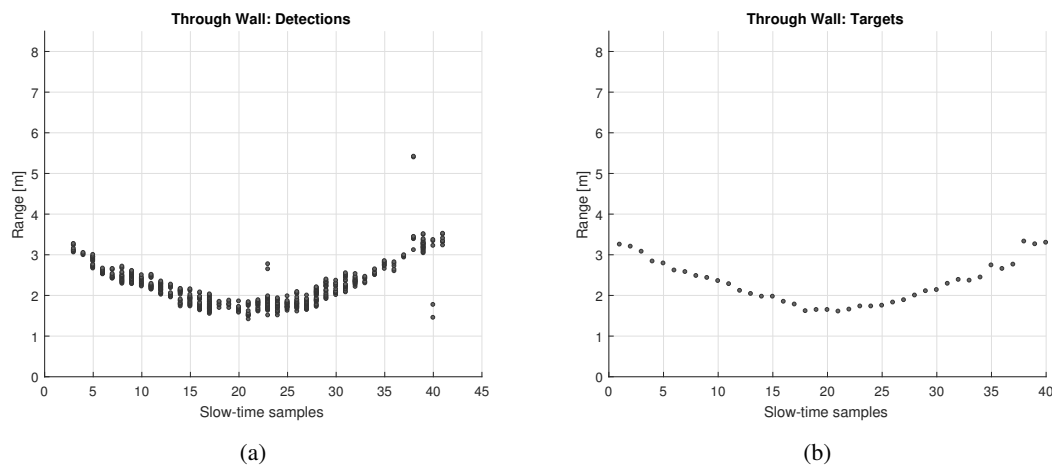


Fig. 7.14: The results of applying (a) the LO-CFAR algorithm and (b) the detection clustering algorithm to the radar range image of Fig. 7.13.

## 7.4 Small Target Detection

In order to test if the system is capable of detecting smaller targets, a measurement is made with a small vehicle as the target. The vehicle is a remote-controlled, 18x13x11 cm plastic car. Because material of the vehicle is mainly plastic, which is not a good reflective material, and because the dimensions of the car are so small, a layer of aluminium foil is attached to the top and side of the vehicle to improve the ability to detect the vehicle. The radar range image of this measurement is given in Fig. 7.15. A pulse integration index of 11 is used, which in situations involving persons would have a maximum reliable range of 10 metres. However, because of the size of the target, the received reflections have a considerably lower intensity compared to situations including a person. It is also important to note that the height of the radars is not adjusted, which means that the target vehicle is not in the same plane as the sensing system. This may result in lower received signal intensities due to the directivity of the antenna. At a distance of 4 m, the vehicle is already difficult to see in the image. Regardless, the detection algorithm is applied to the data to see whether the vehicle is visible.

The results of applying the detection algorithm and detection clustering to the measurement data are shown in Fig. 7.16a and Fig. 7.16b respectively. It is immediately visible that a significant part of the path has been missed by the detection algorithm. In the results, nine consecutive detections are missed, which is not in accordance with the requirement posed by the tracking module. In order to track small targets with a high detection accuracy, a higher pulse integration index is required, which will provide more reliable results at larger ranges. However, this will also result in a lower slow-time sampling frequency.

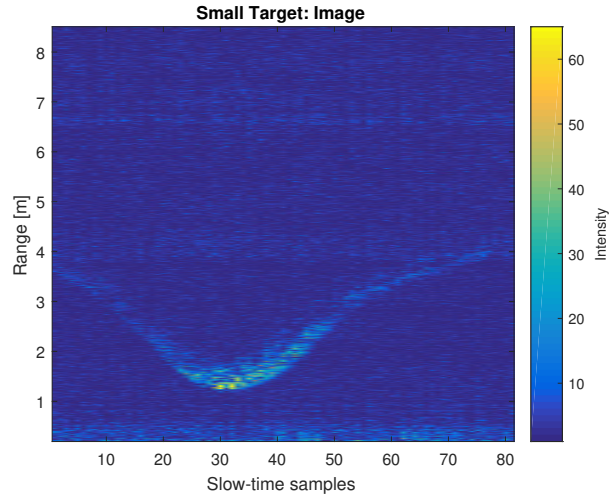


Fig. 7.15: Radar range image of an RC vehicle driving towards and away from the radar.

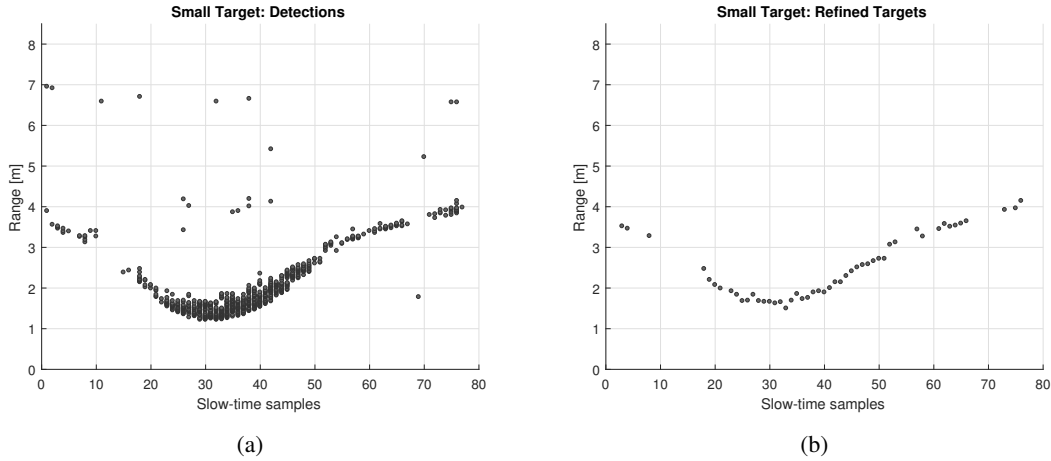


Fig. 7.16: The results of applying (a) the LO-CFAR algorithm and (b) the detection clustering algorithm to the radar range image of Fig. 7.15.

## 7.5 Results of the Complete System

After combining the detection module and the tracking module, the complete system can be tested. In the test measurement, a 6x8 m field is enclosed by four radar modules, and a single person walks on the path illustrated in Fig. 7.17. The maximum range of the radars was increased to 10m to allow detections in the full area of interest. After detection and localisation of the target, the track of the target is filtered, as discussed in [1]. Figure 7.18 shows the results of the measurement.

In the figure, it is visible that the system is accurate on the straight lines. However, the tracking results has a larger deviation from the actual walked pattern at the corners. This is likely caused by three things. The first reason is that the person rounded the corners of the path during walking, and that the person is not a point target, but rather a distributed scatterer, which causes many different reflections. The other reason is that the tracking algorithm smooths the track, causing the corners to be rounded slightly. Finally, the error in localisation will increase for larger distances from the radar, such as in the corners of the track. This error is due to the inherently larger error in localisation at larger distances, and due to the lower amplitude of reflection of the target, resulting in a lower signal-to-noise ratio in the radar signal at this distance.

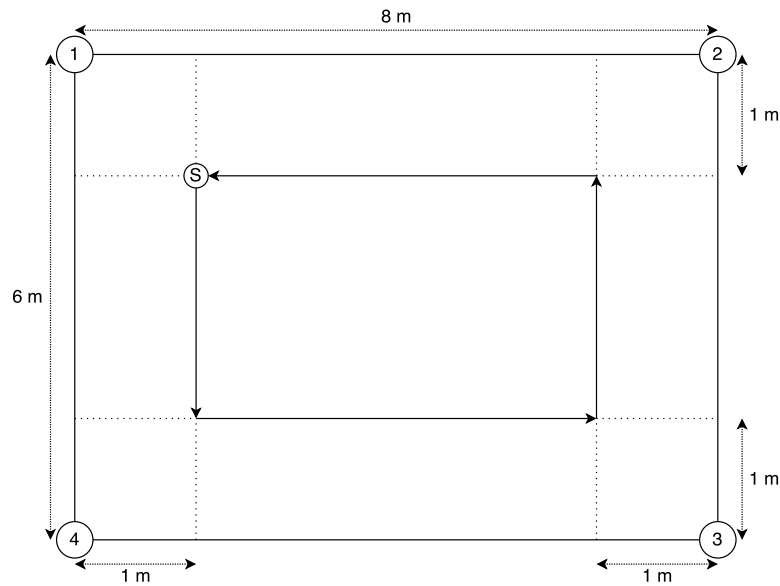


Fig. 7.17: Target track to be measured by the complete tracking system.

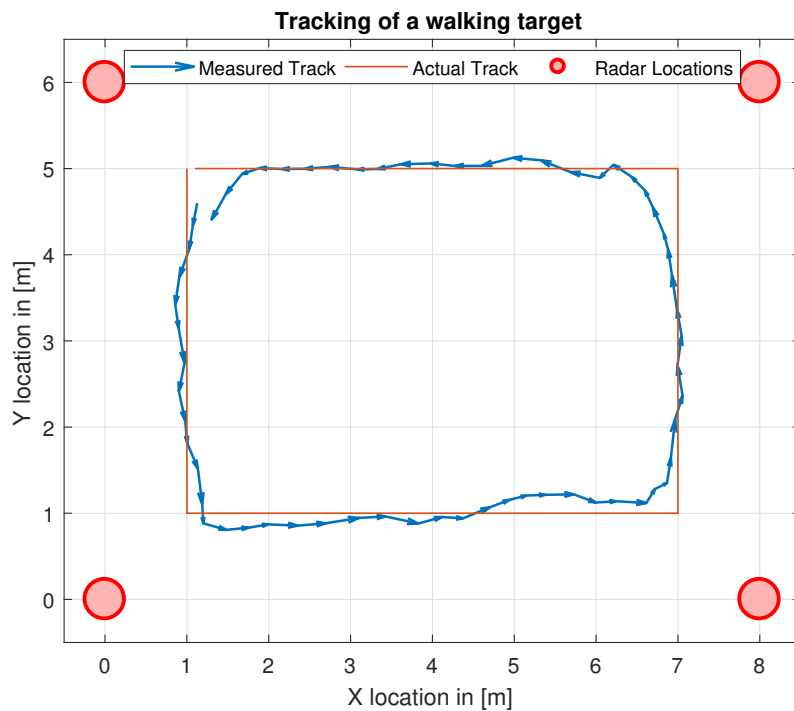


Fig. 7.18: Tracking results of the complete system. The red line represents the actual target location at each point in time and the blue line represents the corresponding system localisation.

Since the error in the corners is much higher than the error in the straight lines, the accuracy for both is evaluated separately. The straight line region is defined as the region up to 0.5 m from the corner of the track. The maximum deviation from the expected location in this region is 30 cm, with a mean deviation of 13 cm. In the corners, the deviation from the expected location is higher, up to 54 cm in the top right corner.

## 7.6 Result Discussion

From the results, it can be concluded that 9 out of 10 of the user requirements are met. A single control unit operates the sensing system, handles the signal processing, and does not require user interaction after set-up. The system is able to detect two persons in an area of interest at a sample rate of 11.2 Hz, as long as the total signal processing time does not exceed the time required to measure. The detection algorithm requires a total of 6 ms for the four radars, and the detection clustering algorithm requires an additional 20 ms to calculate the distance from each radar to the person(s) present in the area. The signal processing for detection is significantly less than the measurement time with the used PII, which means that the refresh rate will depend only on the measurement time, assuming that the tracking algorithm also has a low execution time. Persons can be detected through walls and in cluttered areas. With a pulse integration index of 11 or higher, reliable detections can be made up to a range of at least 10 metres, and therefore, an area of 6x6 metres can be covered. Setup requires placement of the sensors, setting up connections and performing a short calibration with 30 measurements of the background, all of which can be done within 15 minutes. The peak power consumption of the entire sensing system is 17 W, as discussed in Section 3.1.

By comparing the walking patterns of each measurement to the result of the detection clustering algorithm, it is concluded that the sensing system does not always detect the exact position of the target. This can be explained by the fact that the radar senses the person as a large and broad target, making it difficult to determine the exact centre of the person. For example, when a person is walking, the arms and legs move at different positions and speeds with respect to the body of the person. It is therefore difficult to determine whether the user requirement for location accuracy is met based on the detection results only. This means that the user requirement for location accuracy can be met if a good localisation algorithm is implemented, which is discussed in [1].

The detection accuracy of the algorithms is tested and discussed for each situation. For single person detection, the detection accuracy requirement is satisfied in both open and cluttered areas. In the measurements with two persons, the detection accuracy could only be realised in the open area. Two persons in a cluttered area resulted in multi-path reflections that were too significant to successfully detect both persons. Because of this, the person furthest away from the radar cannot be detected reliably. In the through-wall measurement, the detection accuracy was high enough to satisfy the user requirement of through-wall tracking. For a small target, the maximum reliable range is significantly lower than for person detection. However, as long as the execution time of the data acquisition and signal processing does not exceed 200 ms, the pulse integration index can be increased to a maximum of 13, in order to increase the range for which the small target should be reliably detected.

Range-Doppler processing was unable to meet the required velocity estimation. This means that a different method for velocity estimation has to be used in order for the complete system to satisfy user demands. Other methods for velocity estimation are described in the tracking module. [1]

The measurement using the complete system shows that the system is capable of successfully detecting, localising and tracking a target in a 6x8 m area. The mean error in position for the straight line is 13 cm, which meets the user requirements. However, the error in the corners is too high, so the accuracy in those situations must be improved to meet the user requirements for every location of the target.

# Chapter 8

## Conclusion

In order to realise an indoor person tracking system, the user demands and requested functionality of the system have been transferred into technical specifications of the system. Based on an analysis of the available sensing technologies, the ultra-wideband microwave radars have been selected as the optimal sensors for this application, because of the high range resolution obtained from their large bandwidth. In accordance with the required frequency band, and based on the state-of-the-art analysis, the Time Domain<sup>®</sup> PulsON<sup>®</sup> 410 ultra-wideband radar has been selected as the sensor, due to its availability, high spatial accuracy, and its ability to detect targets through walls. The radar module has a bandwidth of 2.2 GHz and a centre frequency of 4.2 GHz, which meets the technical requirements of the sensors. Code channels are used to minimise interference between different sensors. The transmit power was determined to be -12.64 dBm. A minimum number of four sensors are required to prevent ambiguity of location in situations with two targets. The number of sensors in the system was decided to be four, although more sensors can be added to the system to improve accuracy and reliability. Vivaldi antennas are used to transmit the waves, due to their superior directivity over dipole antennas. In the experimental trials, the parameters of the PulsON system have been set according to Table IV. With a PII of 11, a refresh rate of 11.2 Hz can be achieved.

Table IV: Used parameters for the PulsON<sup>®</sup> sensors.

Parameter	Value
Pulse Integration Index	11
Transmit Gain	63 (-12.64 dBm)
Range	0 - 8.5 m

For this sensor, data acquisition and signal processing software has been developed which can detect a moving target and their distance from the radar, based on the received reflections of the transmitted wave. A user interface is implemented from which the parameters of the sensing system can be controlled. The system can operate continuously. In order to reject static clutter in the received signal, background rejection and a fourth-order FIR motion filter are used. Several detection algorithms are compared, of which LO-CFAR is found to have the best performance for real-time tracking applications, due to its robustness, low execution time and excellent detection accuracy, and is therefore integrated in the final detection system. The LO-CFAR algorithm was shown to be an improvement over conventional detection algorithms. Range-Doppler processing was proposed as a method to determine the velocity of a target. However, with the required pulse integration index, it is not feasible to implement Range-Doppler processing in real-time tracking applications, because the velocity of the target cannot be coherently determined due to aliasing of the Doppler shift frequency.

## 8.1 Reflection on Results

Based on a comparison between the results and discussion in Chapter 7 and the programme of requirements given in Chapter 2, it can be concluded that with the current system, most of the functional requirements of the system are met. With the hardware communication, signal processing and target detection combined, a detection system has been developed which can be used in real-time applications. The detection system can be used as a module in a target tracking system to localize a moving target and maintain its path. Using the chosen radars, it is possible to detect a single target in both open and cluttered areas, but its reliability and accuracy suffer slightly from multi-path reflections in a cluttered area. Through-wall detection of targets is possible, although this requires a higher pulse integration index than measurements without direct obstacles in front of the radar. The higher pulse integration index affects the maximum sample frequency of the system, which effectively lowers the quality of the final system by reducing the locations per second that are provided.

Difficulties arise when multiple persons are to be detected by the system. In open areas, the detection algorithm can still clearly detect two targets, as long as the targets do not get too close to each other. In cluttered areas however, the two targets combined cause too many multi-path reflections, which often makes the target furthest from the radar undetectable. Two persons were visible for only a small section of the measurement. Multi-person detection in cluttered areas is a great problem of interest, as other types of tracking systems have issues in these environments such due to for example loss of line-of-sight, and as a result, the problem of multiple person tracking in cluttered environments will have to be further investigated.

Range-Doppler processing, which was proposed as a technique to determine the velocity of the target, has been shown to work using simulations of a moving target. In a tracking system, a velocity estimation could prove to be useful. However, due to the low slow-time sampling frequency of the system, a maximum velocity of  $0.18 \text{ m s}^{-1}$ , which is significantly lower than the maximum velocity requested by the user. Other methods to estimate velocity, such as using information from the track of the target, are discussed in [1].

## 8.2 Future Work and Recommendations

**Testing more directional antennas.** It may be beneficial to use more directional antennas for certain tracking applications. Multi-path effects can be further reduced by using antennas with a directivity that limits the signal to the area of interest. Through-wall tracking applications can also benefit from more directional antennas by using the transmitted energy more effectively.

**Implementing and testing a multi-static radar system.** Instead of transmitting and receiving individually for all radars, a system could be designed that uses one transmitter and multiple receiver. By transmitting and receiving from different positions, detection of targets are possibly simplified, as each radar will view the area from multiple perspectives. This allows for a more decentralised system. A multi-static radar system would also allow the radars to determine their own position relative to each other. Because the radar locations would no longer need to be entered manually, this would decrease set-up time. Because the radar locations would more accurately correspond to their focal points, the radar locations would also likely be more accurate, resulting in more accurate detections.

**Implementing more complex detection algorithms.** In this report, only a few detection algorithms have been considered. With more complex algorithms, the detection accuracy may be increased, resulting in more accurate target detection and tracking. For example, there are more complex variants of the CFAR algorithm which take the statistics of the background into account.

**Additional filtering of the radar data.** In order to improve the signal-to-noise ratio and make detection easier, additional filtering could be applied to the radar data. For example, a bandpass filter could be designed to remove noise outside the specified bandwidth of the radars, as there is no signal information

contained in frequencies outside of this bandwidth.

**Implementing a neural network for person detection.** Neural networks have the ability to optimise the parameters used in the detection algorithms, or to replace the detection algorithm altogether. The neural network can be used to analyse data and detect patterns in data which are difficult to detect by humans. These patterns can be used to optimise a detection system based on training data provided by the user.



# **Appendices**



## Appendix A

# Range Measurements

Table V shows the distances to a metal plate as measured with a laser measure and the same distances as measured with a radar module. From this data, the range accuracy of the radar system can be estimated.

Table V: Accuracy measurement of the P410 radar module.

<b>Laser Measured Range [m]</b>	<b>Radar Detected Range [m]</b>
2.36	2.30
3.62	3.53
4.29	4.19
5.07	5.00
6.15	6.07
7.21	7.19
5.23	5.05
2.74	2.66
1.47	1.39
1.61	1.56
2.64	2.51
3.10	2.96
3.57	3.51
3.97	3.88
4.55	4.50
5.65	5.55
6.94	6.81
7.37	7.29



## Appendix B

# Velocity Estimation Using Range-Doppler Information

To obtain the radial velocity of the target with respect to one radar, a unit vector is taken in the direction from the radar to the target. This unit vector is then scaled by the relative velocity in that direction, as measured by the range-Doppler algorithm. If a perpendicular line is drawn from the endpoint of this velocity component, any point on this line could be the endpoint of the two-dimensional target velocity vector. This is shown in Fig. B.1.

To narrow down the options for the target velocity, a second radar must be used. This second radar generates its own velocity component, with its corresponding line of possible target velocity endpoints. If the radar velocity components are linearly independent, these two lines will intersect at one certain point, as shown in Fig. B.2. This intersection is then the endpoint of the target's two-dimensional velocity vector.

This problem can be solved with linear algebra. Equation B.1 shows the equation that describes the target velocity vector for each radar.  $\mathbf{v}_n$  represents the velocity component of radar  $n$ ,  $\mathbf{v}_0$  represents the real two-dimensional target velocity, and  $\hat{\mathbf{v}}_{\perp n}$  represents a unit vector perpendicular to  $\mathbf{v}_n$ .  $\lambda_n$  represents an arbitrary real number to scale this perpendicular unit vector by, so that the sum of the two vectors equals  $\mathbf{v}_0$ .

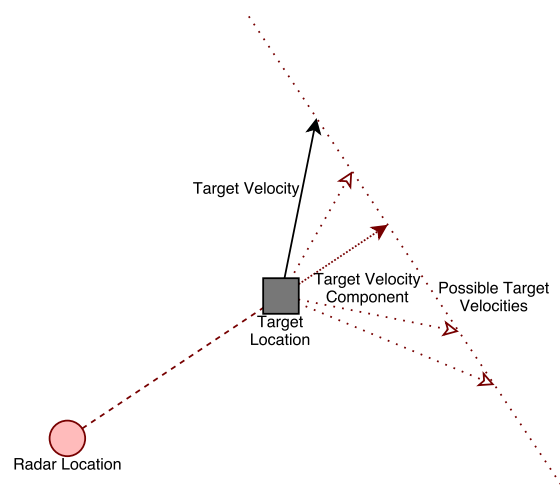


Fig. B.1: Diagram showing possible target velocities from a single Range-Doppler measurement. The dotted line perpendicular to the velocity component represent every possible endpoint of the target's velocity vector.

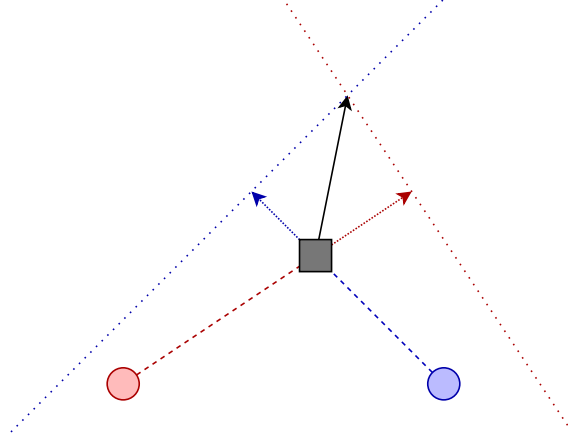


Fig. B.2: Diagram showing the velocity resulting from the intersection of the velocities from two Range-Doppler measurements.

$$\mathbf{v}_n + \lambda_n \hat{\mathbf{v}}_{\perp n} = \mathbf{v}_0 \quad (\text{B.1})$$

This equation can be extended to form the matrix multiplication seen in Eq. B.2 and Eq. B.3.

$$X = H^\dagger Y \quad (\text{B.2})$$

$$H = \begin{pmatrix} -v_{1,y} & 0 & \dots & 0 & 1 & 0 \\ v_{1,x} & 0 & \dots & 0 & 0 & 1 \\ 0 & -v_{2,y} & \dots & 0 & 1 & 0 \\ 0 & v_{2,x} & \dots & 0 & 0 & 1 \\ \vdots & \vdots & \ddots & \vdots & \vdots & \vdots \\ 0 & 0 & \dots & -v_{N,y} & 1 & 0 \\ 0 & 0 & \dots & v_{N,x} & 0 & 0 \end{pmatrix}; X = \begin{pmatrix} \lambda_1 \\ \lambda_2 \\ \vdots \\ \lambda_n \\ v_{0,x} \\ v_{0,y} \end{pmatrix}; Y = \begin{pmatrix} v_{1,x} \\ v_{1,y} \\ v_{2,x} \\ v_{2,y} \\ \vdots \\ v_{N,x} \\ v_{N,y} \end{pmatrix} \quad (\text{B.3})$$

In these equations,  $v_{x,0}$  and  $v_{y,0}$  are the x and y components of the target velocity.  $v_{n,x}$  and  $v_{n,y}$  are the x and y components of the target's relative velocity in the direction of radar  $n$ , with  $n \in \{1, 2, \dots, N\}$ , where  $N$  is the total number of radars.  $H^\dagger$  denotes the pseudo-inverse of the rectangular matrix  $H$ . From  $X$ , the target's two-dimensional velocity vector can be determined.

# Bibliography

- [1] Q. Bruinsma *et al.*, *Target Localisation And Tracking In A UWB Radar Network*, Delft University of Technology Std., June 2017.
- [2] X. Tong *et al.*, “Artificial potential field based cooperative particle filter for multi-view multi-object tracking,” in *2013 International Conference on Virtual Reality and Visualization*, Sept 2013, pp. 74–80.
- [3] P. H. Chang and C. H. Shen, “A new fast infrared tracking system with thermopile array implementation,” in *2007 IEEE/LEOS International Conference on Optical MEMS and Nanophotonics*, Aug 2007, pp. 97–98.
- [4] T. Mori *et al.*, “Multiple people tracking by integrating distributed floor pressure sensors and rfid system,” in *2004 IEEE International Conference on Systems, Man and Cybernetics (IEEE Cat. No.04CH37583)*, vol. 6, Oct 2004, pp. 5271–5278 vol.6.
- [5] Q. Liu *et al.*, “Person tracking using audio and depth cues,” in *2015 IEEE International Conference on Computer Vision Workshop (ICCVW)*, Dec 2015, pp. 709–717.
- [6] H. S. Amaresh *et al.*, “Real-time intruder detection system using sound localization and background subtraction,” in *2014 Texas Instruments India Educators’ Conference (THIEC)*, April 2014, pp. 131–137.
- [7] F. Schler *et al.*, “Person tracking in three-dimensional laser range data with explicit occlusion adaption,” in *2011 IEEE International Conference on Robotics and Automation*, May 2011, pp. 1297–1303.
- [8] J. Cui *et al.*, “Fusion of detection and matching based approaches for laser based multiple people tracking,” in *2006 IEEE Computer Society Conference on Computer Vision and Pattern Recognition (CVPR’06)*, vol. 1, June 2006, pp. 642–649.
- [9] K. Chawla *et al.*, “Object localization using rfid,” in *Wireless Pervasive Computing (ISWPC), 2010 5th IEEE International Symposium on*. IEEE, 2010, pp. 301–306.
- [10] Narrow-beam radar. [Online]. Available: <https://en.wikipedia.org/wiki/Radar>
- [11] B. Gulmezoglu *et al.*, “Multiperson tracking with a network of ultrawideband radar sensors based on gaussian mixture phd filters,” *IEEE Sensors Journal*, vol. 15, no. 4, pp. 2227–2237, April 2015.
- [12] J. Li *et al.*, “Through-wall detection of human being’s movement by uwb radar,” *IEEE Geoscience and Remote Sensing Letters*, vol. 9, no. 6, pp. 1079–1083, Nov 2012.
- [13] A. Lin and H. Ling, “Through-wall measurements of a doppler and direction-of-arrival (ddoa) radar for tracking indoor movers,” in *2005 IEEE Antennas and Propagation Society International Symposium*, vol. 3B, July 2005, pp. 322–325 vol. 3B.
- [14] J. Sachs *et al.*, “Detection and tracking of moving or trapped people hidden by obstacles using ultrawideband pseudo-noise radar,” in *2008 European Radar Conference*, Oct 2008, pp. 408–411.

- [15] Y. Aslan, *Person Detection and Tracking in a Networked Ultra-Wideband Radar System*, Delft University of Technology Std., 2015.
- [16] Y. He, “Human target tracking in multistatic ultra-wideband radar,” Ph.D. dissertation, TU Delft, Delft University of Technology, 2014.
- [17] A. Samokhin *et al.*, “Algorithm for multiple targets localization and data association in distributed radar networks,” in *2014 15th International Radar Symposium (IRS)*, June 2014, pp. 1–6.
- [18] Radio spectrum. [Online]. Available: [https://en.wikipedia.org/wiki/Radio\\_spectrum](https://en.wikipedia.org/wiki/Radio_spectrum)
- [19] Relation bandwidth and range resolution. [Online]. Available: <http://www.radartutorial.eu/01.basics/Range%20Resolution.en.html>
- [20] *PulsON<sup>®</sup> 410 Data Sheet*, TimeDomain<sup>®</sup> Std., November 2013.
- [21] *PulsON<sup>®</sup> 400 Broadspec Antenna Data Sheet*, TimeDomain<sup>®</sup> Std., March 2011.
- [22] *Monostatic Radar Application Programming Interface (API) Specification v1.2*, TimeDomain<sup>®</sup> Std., January 2014.
- [23] F. M. Dekking *et al.*, *A Modern Introduction to Probability and Statistics*. Springer, 2005.
- [24] Cfar algorithm. [Online]. Available: <https://nl.mathworks.com/help/phased/examples/constant-false-alarm-rate-cfar-detection.html>
- [25] L. L. Scharf, *Statistical Signal Processing: Detection, Estimation and Time Series Analysis*. Addison Wesley, 1991.
- [26] Y. He *et al.*, “Range-doppler processing for indoor human tracking by multistatic ultra-wideband radar,” in *2012 13th International Radar Symposium*, May 2012, pp. 250–253.
- [27] R. Wolfson, *Essential University Physics Volume 1*. Pearson Education, 2014.
- [28] T. Nagano *et al.*, “Range migration compensation for moving targets with unknown constant velocity in chirp radars,” in *2011 8th European Radar Conference*, Oct 2011, pp. 125–128.